

Hadronic vs e^+e^- colliders

Hadronic machines:

- enormous production of b-hadrons ($\sigma_{b\bar{b}} \sim 50 \mu\text{b}$)
- all b-hadrons can be produced
- trigger is challenging
- complicated many-particles events
- incoherent production of B mesons

$e^+ e^-$ collider at the $Y(4S)$:

- copious production of b-hadrons ($\sigma_{b\bar{b}} \sim 1 \text{ nb}$)
- only B^0 and B^+ can be produced
- trigger is moderately easy
- simple events, all the particles come from B decays
- coherent production of B mesons in a $L=1$ state
- B are produced almost at rest in the $Y(4S)$ rest frame.
Travel $\sim 26 \mu\text{m}$ before decaying in that frame
Solution: use beams of different energies to boost the $Y(4S)$ rest frame w.r.t. the lab frame increasing the spatial separation of the decays making it measurable

KEK-B vs PEP-II

Both started in may/june 1999

KEK-B:

8.0 GeV electrons and 3.5 GeV positrons

$$\beta\gamma = 0.42$$

PEP-II:

9.0 GeV electrons and 3.1 GeV positrons

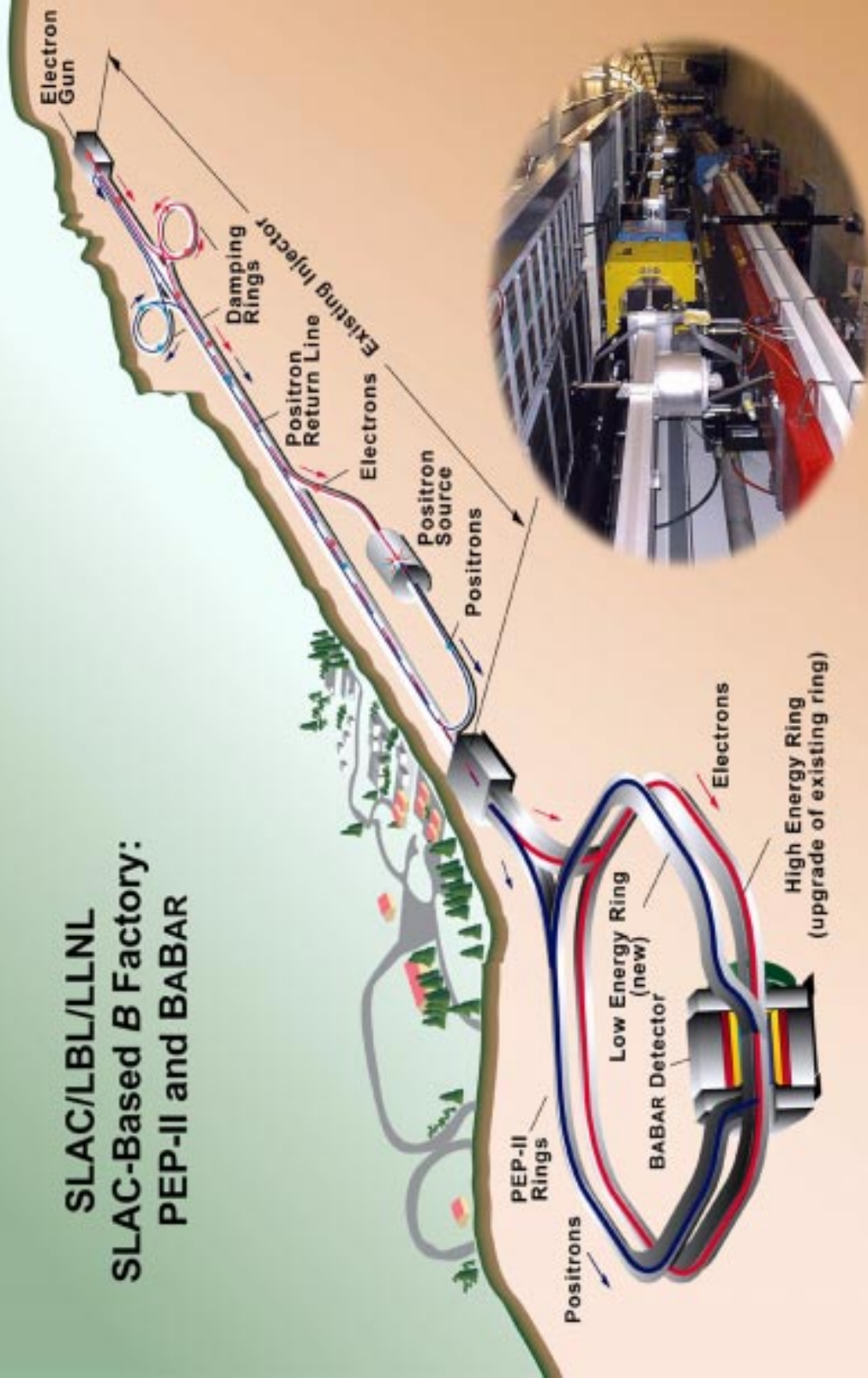
$$\beta\gamma = 0.56$$

mean separation between decay vertices: 260 μm

CM boost:

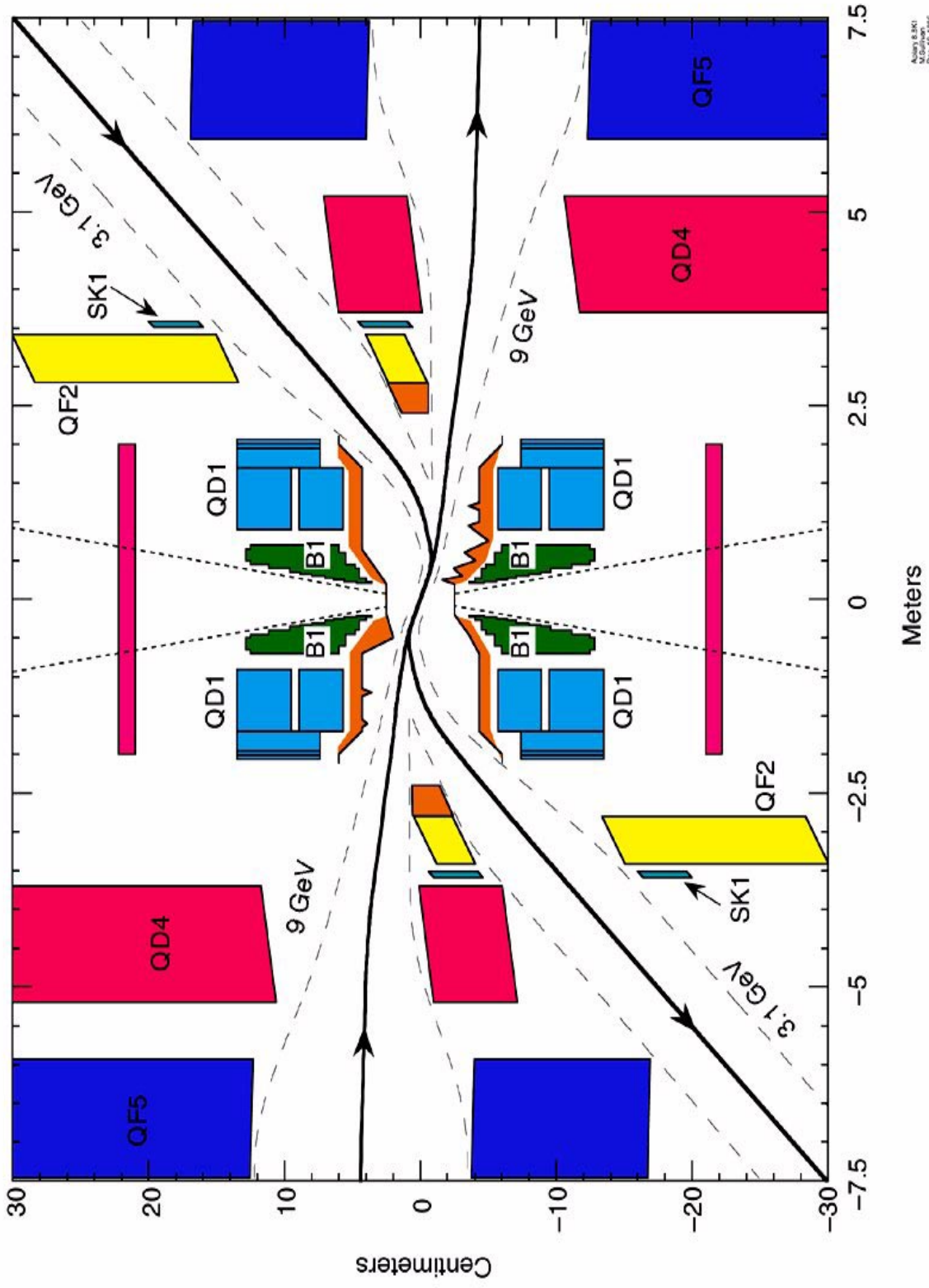
- folds particles forward
- Increases momentum range to cover with Particle ID

SLAC/LBL/LLNL SLAC-Based B Factory: PEP-II and BABAR



Both Rings Housed in Current PEP Tunnel

Interaction Region



PEP-II HER Performance Results

<u>Parameter</u>	<u>Units</u>	<u>Design</u>	<u>Best achieved</u>	<u>Running with BABAR, "typical"</u>
Energy	GeV	9.0	9.0, ramp to 9.1 & back	9.0, ramp 8.84-9.04
Single bunch current	mA	0.6	12	0.75
Number of bunches		1658	1658	829
Total beam current	A	0.75 (1.0)	0.92	0.65
Beam Lifetime		4 hrs @ 1A	11 hrs @ 0.9 A	9 hrs @ 0.65 A
Max. Injection Rate	mA/sec	2.1 @ 60Hz	4.0 @ 15Hz	2.5 @ 15 Hz

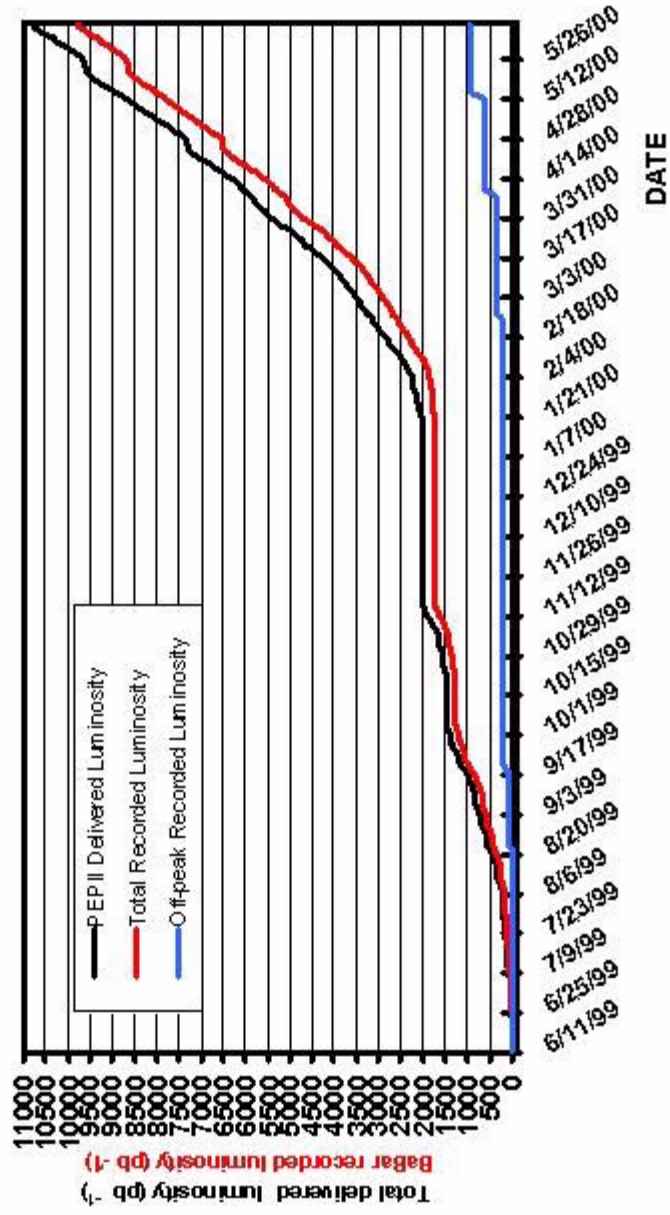
PEP-II LER Performance Results

<u>Parameter</u>	<u>Units</u>	<u>Design</u>	<u>Best achieved</u>	<u>Running with BABAR, "typical"</u>
Energy	GeV	3.1	3.1	3.1
Single bunch current	mA	1.3	7.0	1.2
Number of bunches		1658	1658	829
Total beam current	A	2.1	1.7	1.0
Beam Lifetime		4 hrs @ 2A	3.5 h @ 1 A	3 hrs @ 1 A
Max. Injection Rate	mA/sec	5.9 @ 60 Hz	9.0 @ 30 Hz	4.0 @ 15 Hz

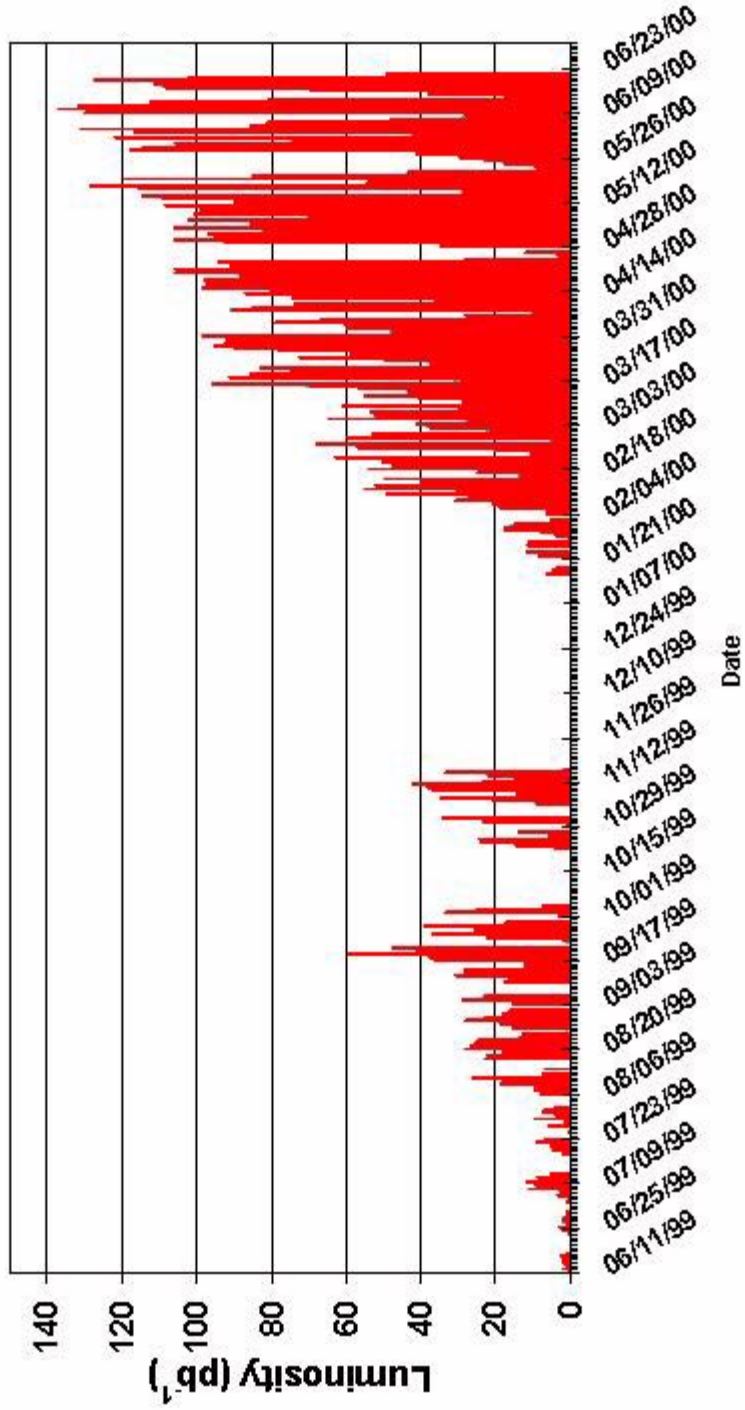


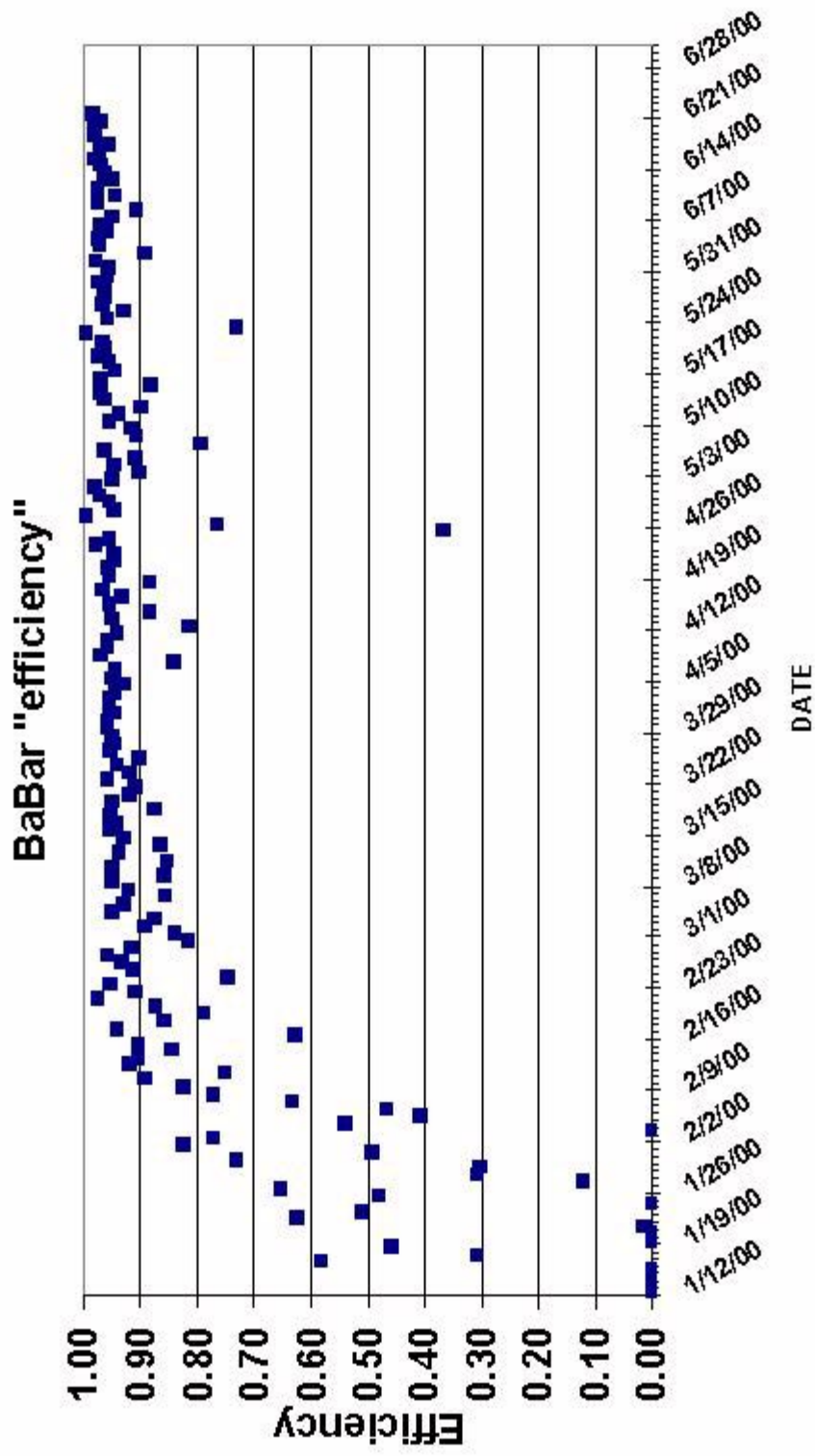
Updated 02/29/2000

BaBar Recorded luminosity - 1999 + 2000

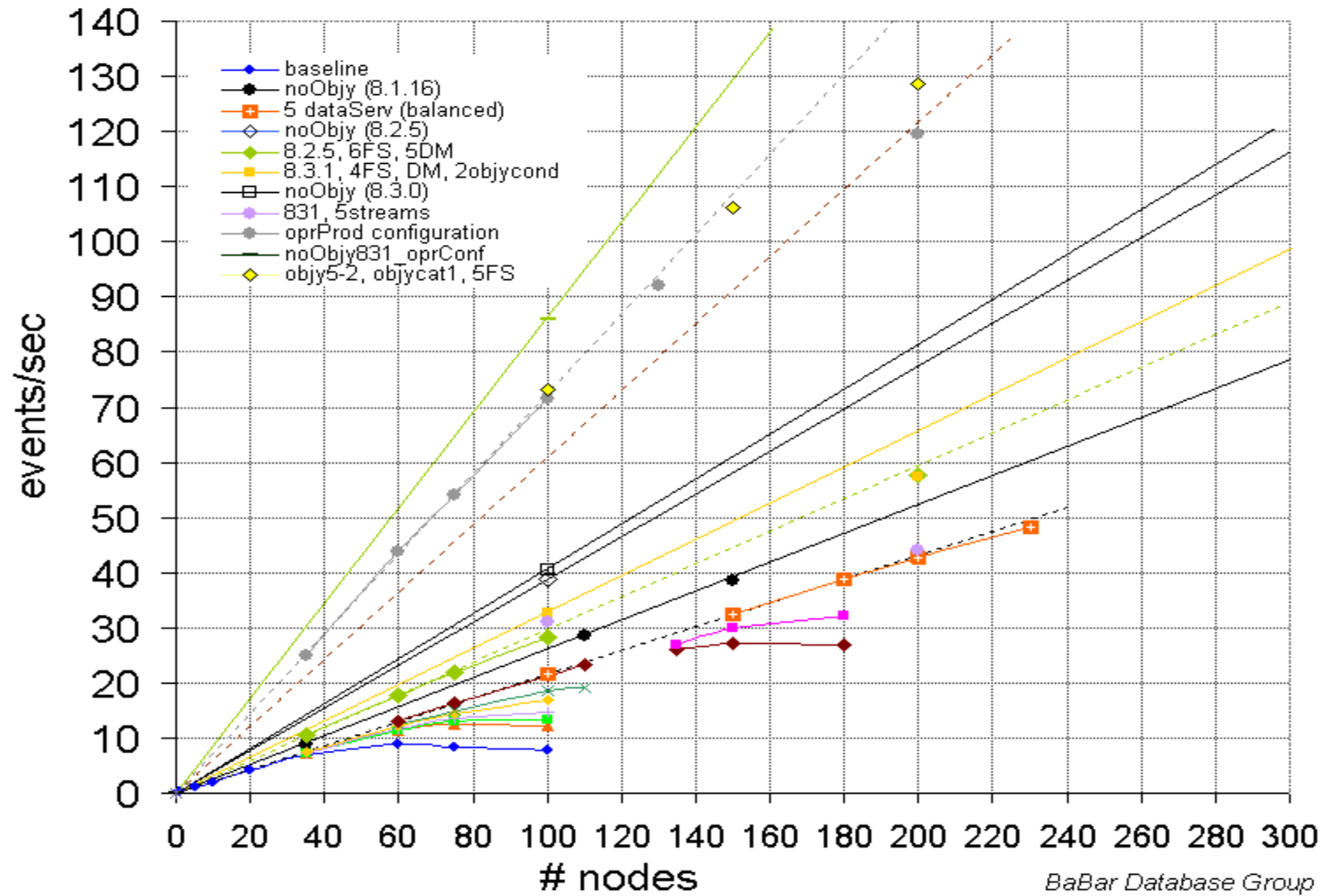


BaBar Daily Recorded Luminosity



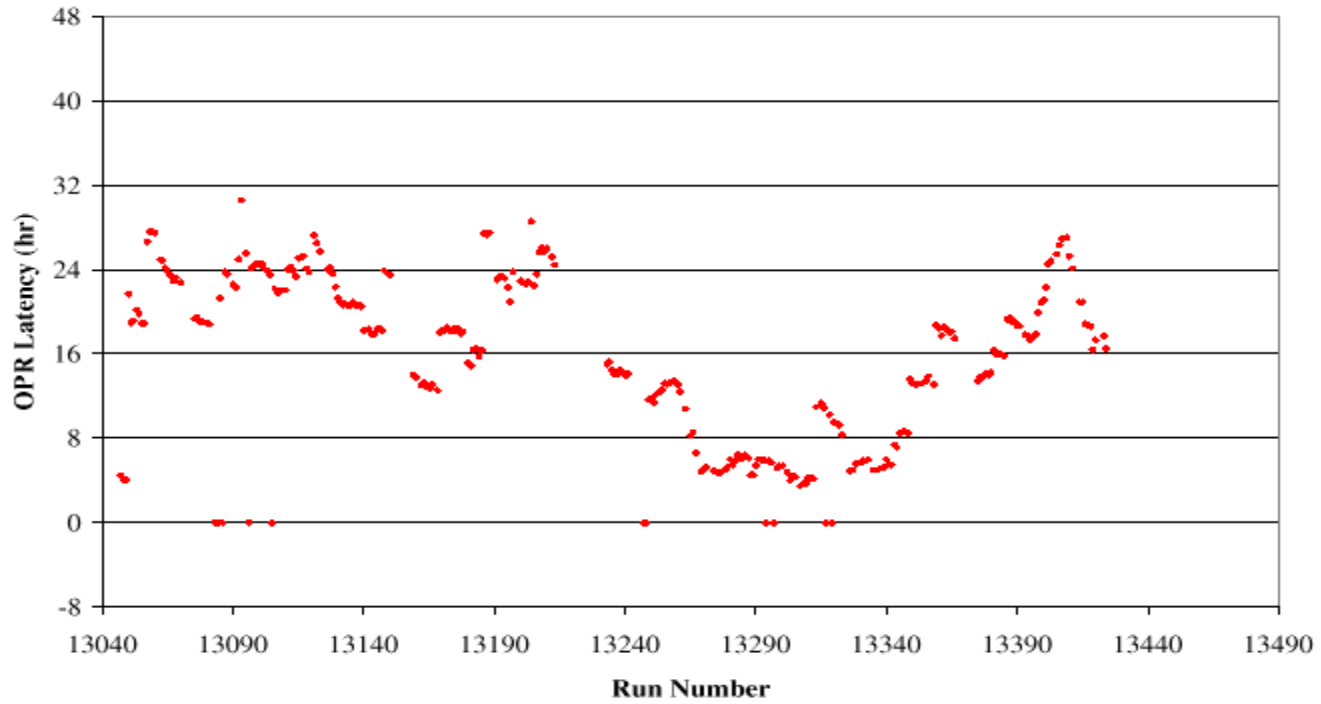


Objectivity Performance & Scalability Tests

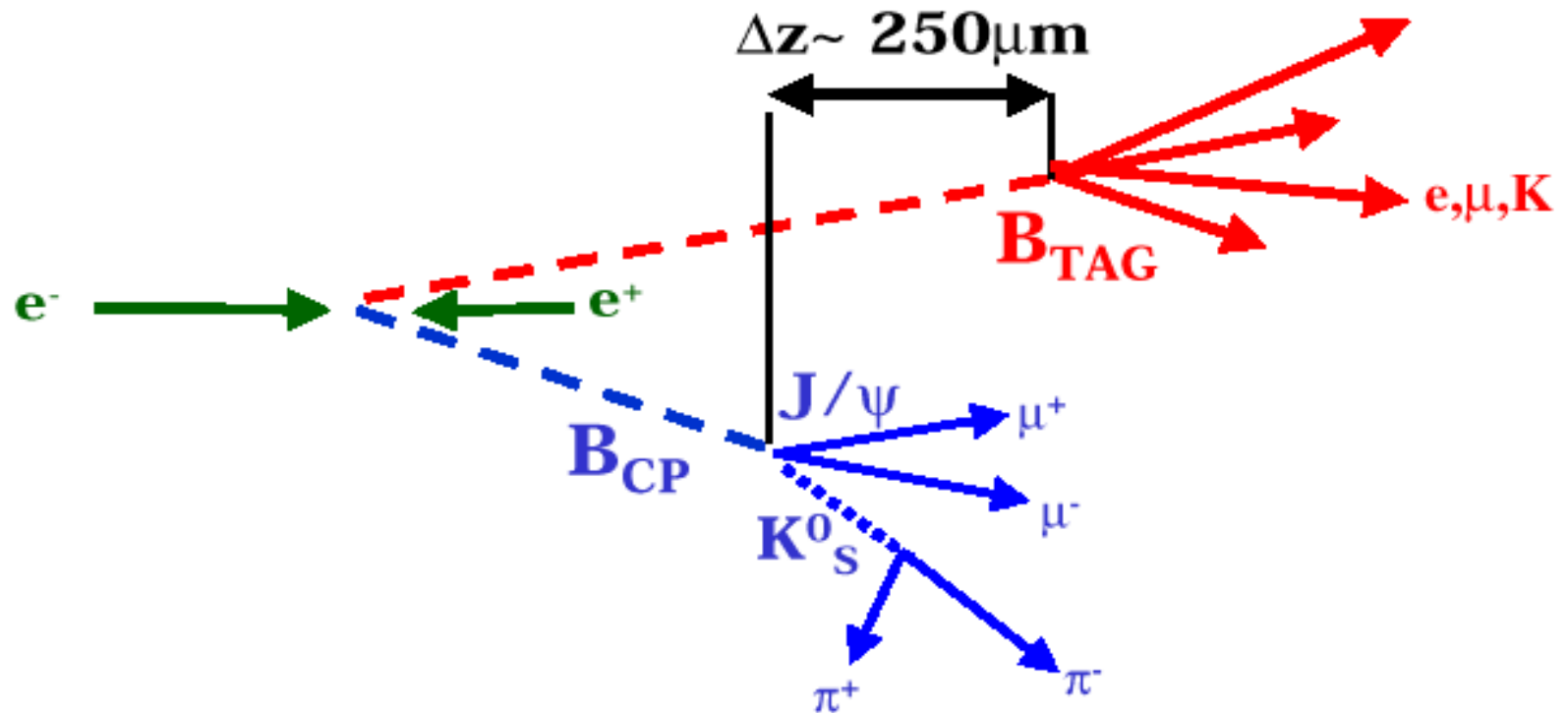


Offline Prompt Reconstruction Latency

May 2000

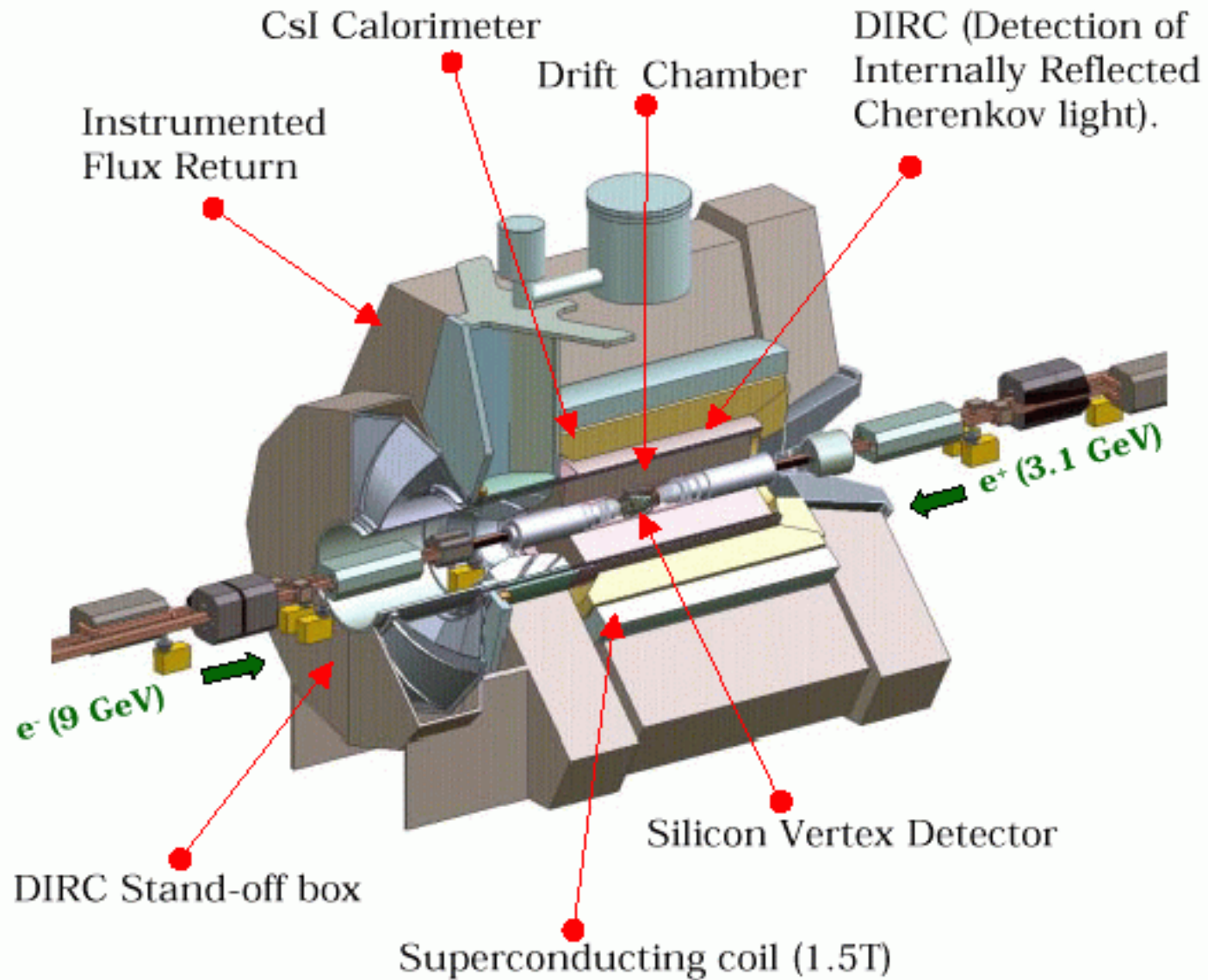


CP violation measurements require:



- Excellent tracking performance and vertex reconstruction.
- Charged particle identification (e, μ, K, π) over large kinematic range.
- Neutral particle reconstruction (γ, π^0, K_L^0).

The BaBar Detector



Silicon Vertex Tracker

Performance Requirements:

- Δz resolution $< 130 \mu\text{m}$
- Single vertex resolution $< 80 \mu\text{m}$
- Stand-alone tracking for $P_t < 100 \text{ MeV}/c$

PEP II Constraints:

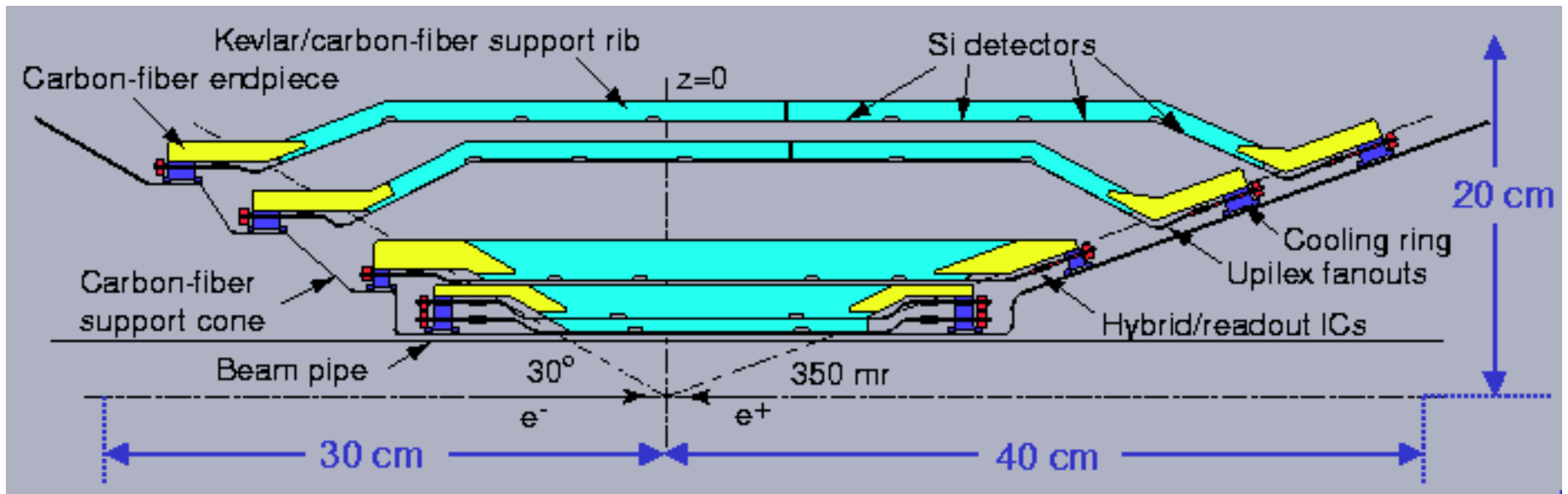
- Dipole magnets (B1) at $\pm 20 \text{ cm}$ from interaction point
- Polar angle: $17.2^\circ < \theta < 150^\circ$
- Bunch Crossing Period 4.2 ns
- Radiation exposure at innermost layer:
average 33Krad/year
in beam plane: 240 Krad/year

5 layers of double-sided AC-coupled Silicon

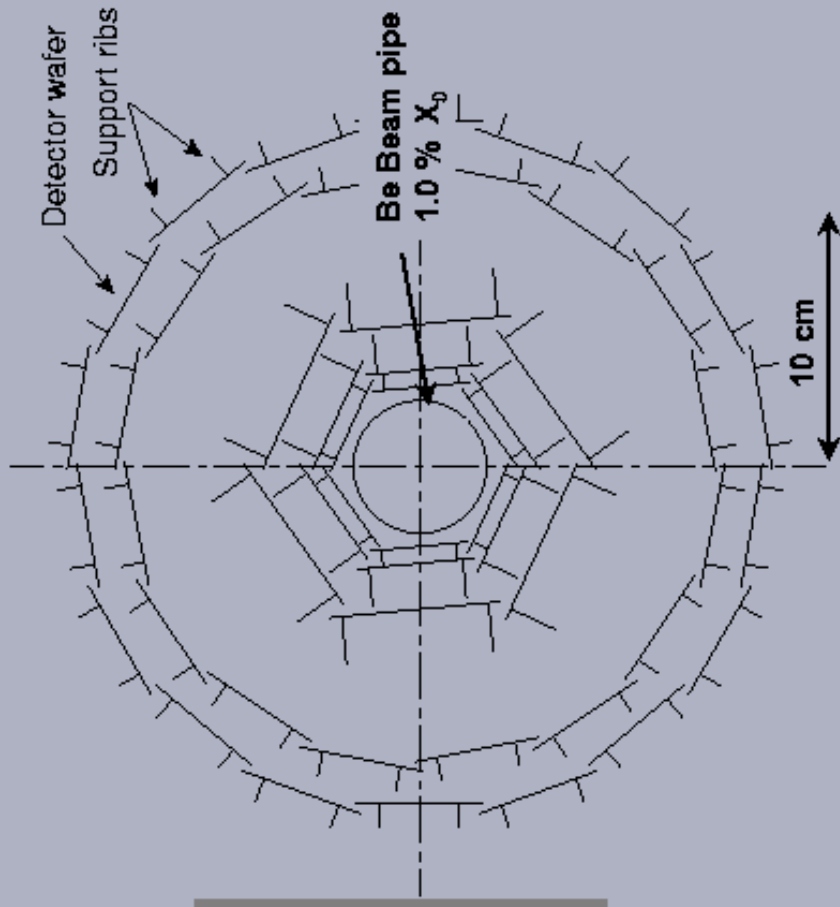
Custom rad-hard readout IC (the AToM chip)

Stand-alone tracking for slow particles:

- inner 3 layers for angle and impact parameter measurement
- outer 2 layers for pattern recognition and low P_t tracking



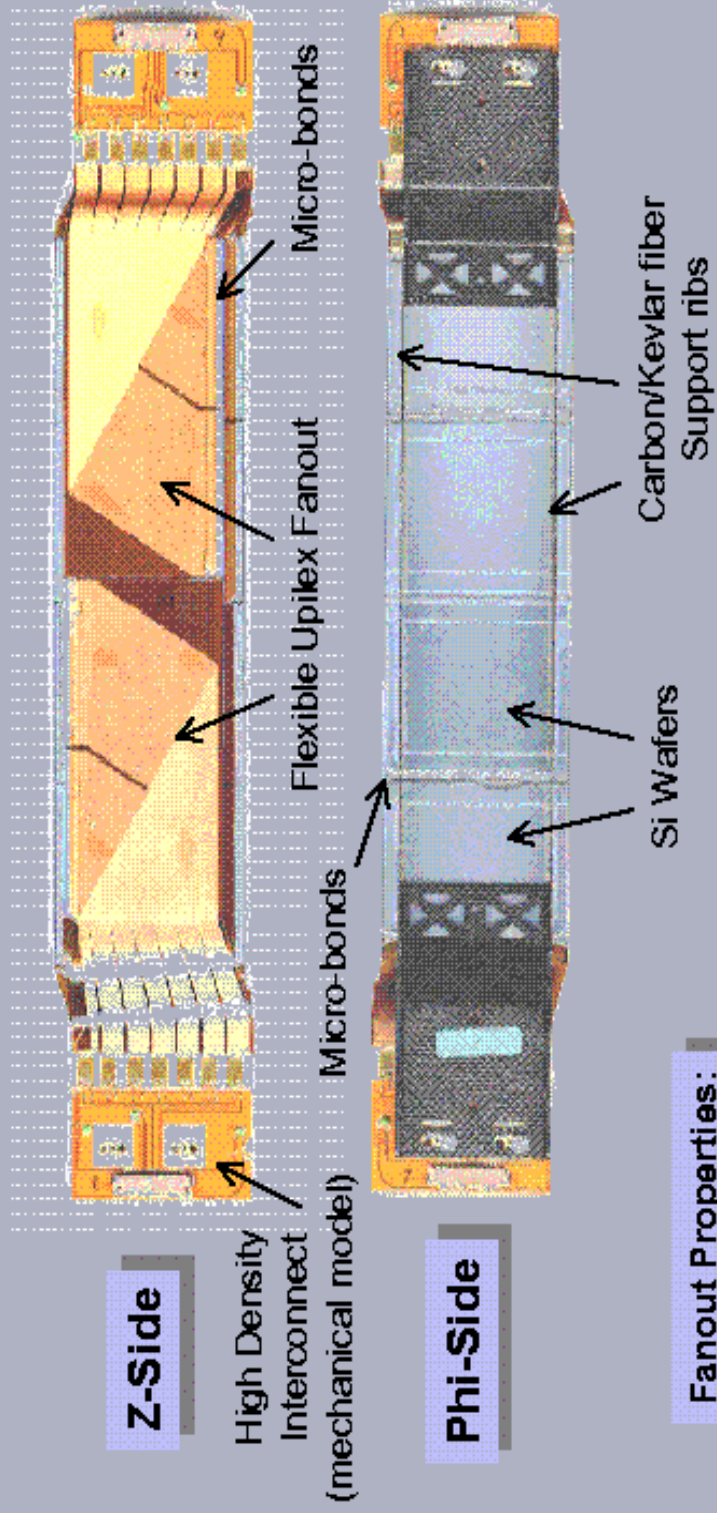
SVT Geometry



<u>Layer</u>	<u>Radius</u>
1	3.3 cm
2	4.0 cm
3	5.9 cm
4	9.1 to 12.7 cm
5	11.4 to 14.6 cm

(Arched wedge wafers not shown)

SVT Modules



Z-Side

High Density Interconnect (mechanical model)

Phi-Side

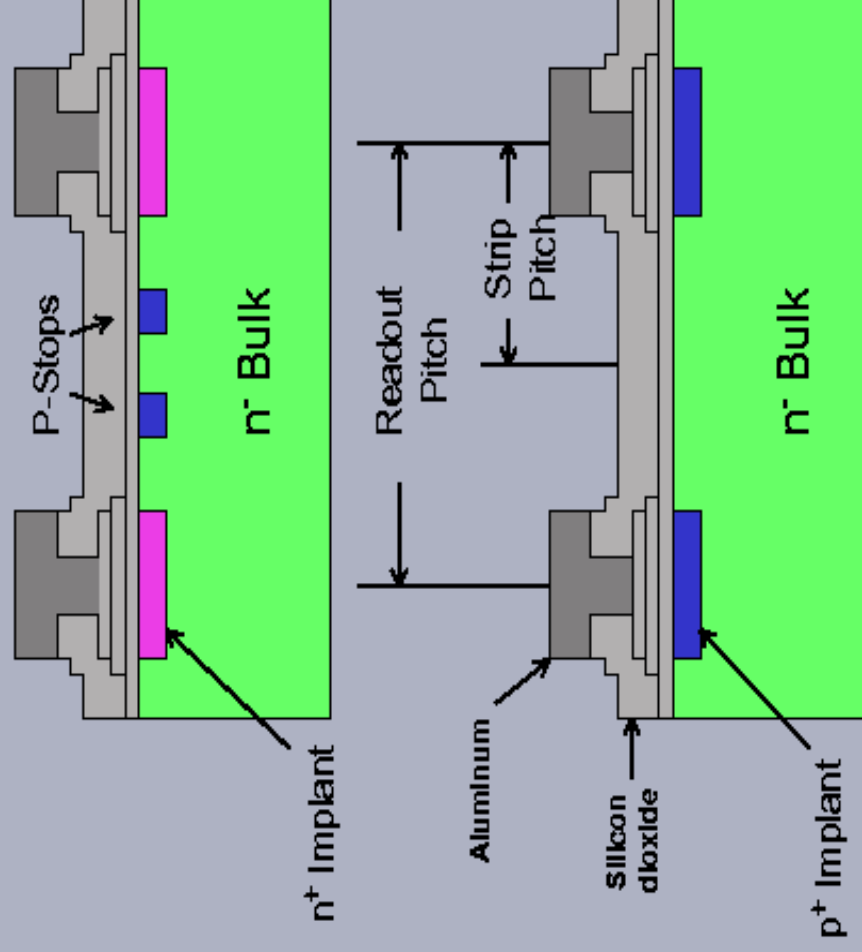
Fanout Properties:

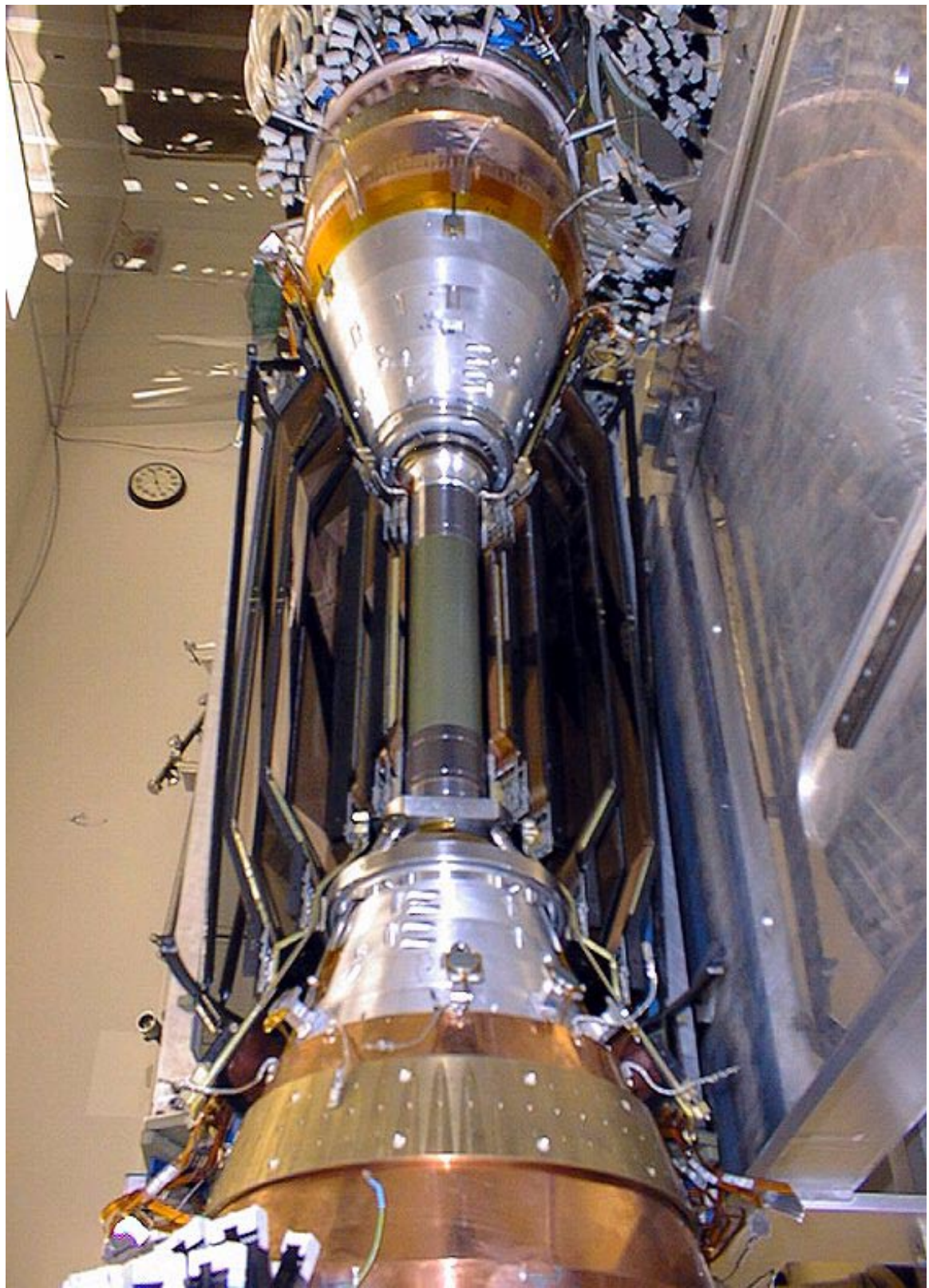
- $< 0.03\% X_0$
- 0.52 pF/cm

Silicon Wafers

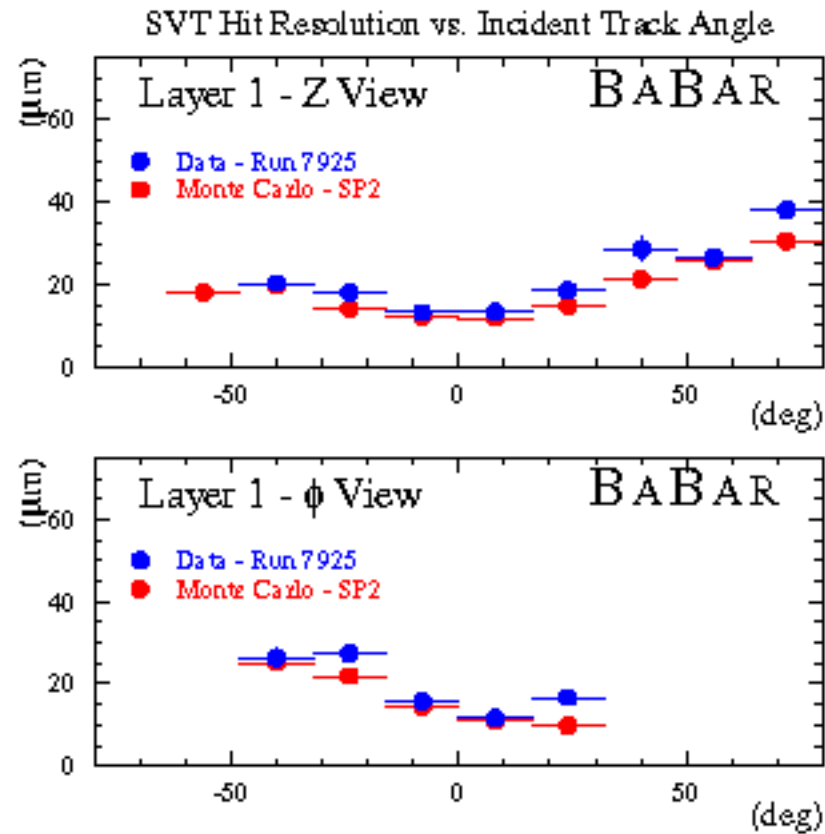
Features:

- Manufactured at Micron.
- 300 μm thick.
- 6 different wafer designs.
- n⁻ bulk, 4-8 k Ω cm.
- AC coupling to strip implants.
- Polysilicon Bias resistors on wafer, 5 M Ω .





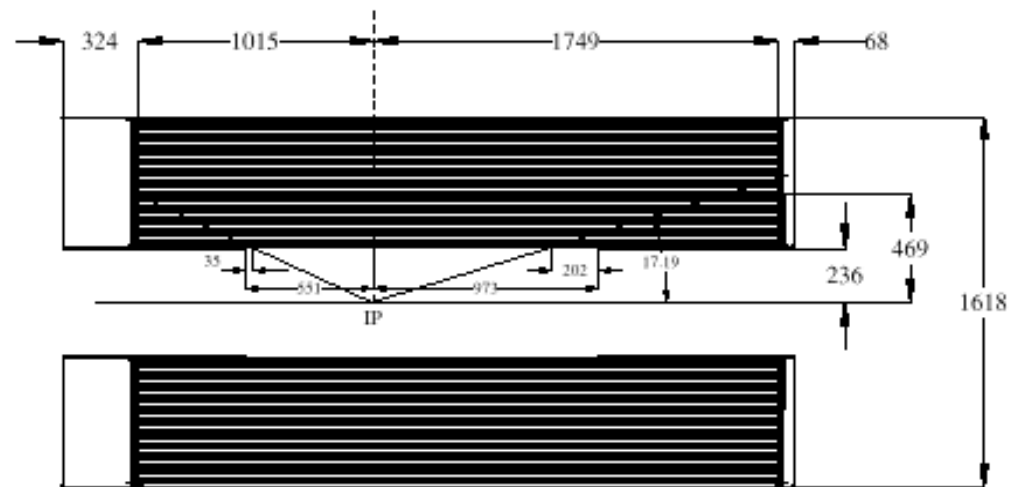
SVT Hit Resolution vs Incident Track Angle



Drift Chamber



Drift Chamber Structure

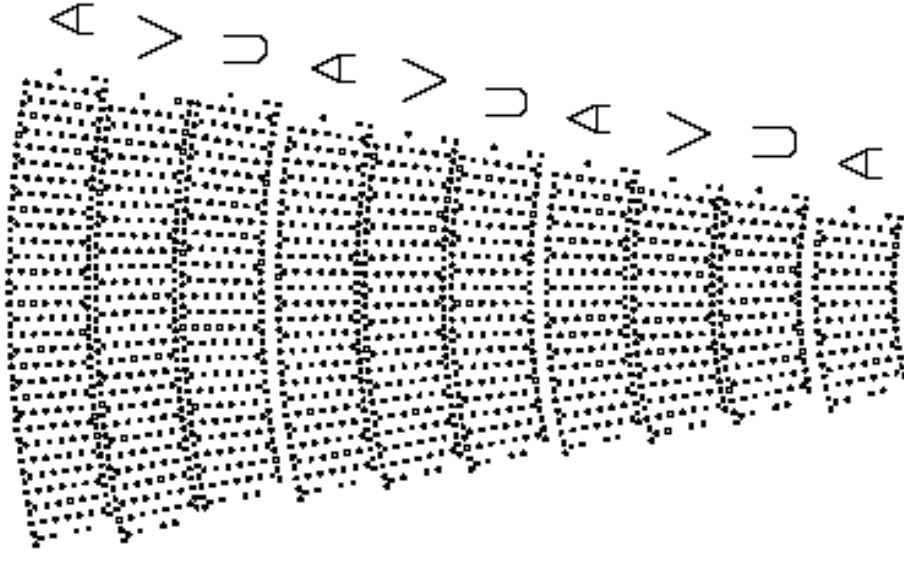


- Flat aluminum rear (24 mm) and forward (24+12 mm) endplates
 - Forward endplate with thin outer section to minimize material
 - Preamplifier and digitizer electronics on rear endplate only
- Load-bearing inner and outer walls to reduce deflections
 - Inner wall of 1 mm-beryllium (40% load)
 - Segmented outer wall of 2x1.5 mm CF skins on Nomex core (60% load)



Drift System Layout

- 40-layer small-cell chamber
 - Cells are 12x18 mm² in size
 - 7104 drift cells with hexagonal field wire pattern
 - 80 and 120 μm gold-plated aluminum field wires
- Layers organized into superlayers with same orientation
 - Wire directions for 4 consecutive layers: axial-u-v-stereo
 - Required for fast reduction of input to Level 1 trigger via segment finding
 - Transition field shaping voltages to maintain reasonably uniform performance

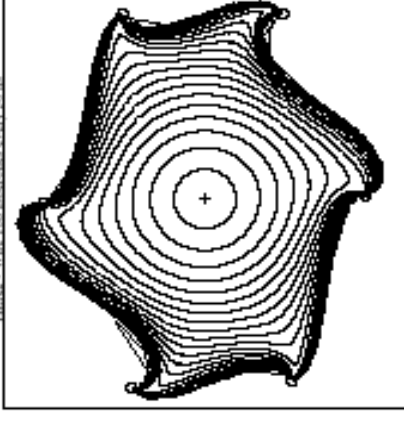


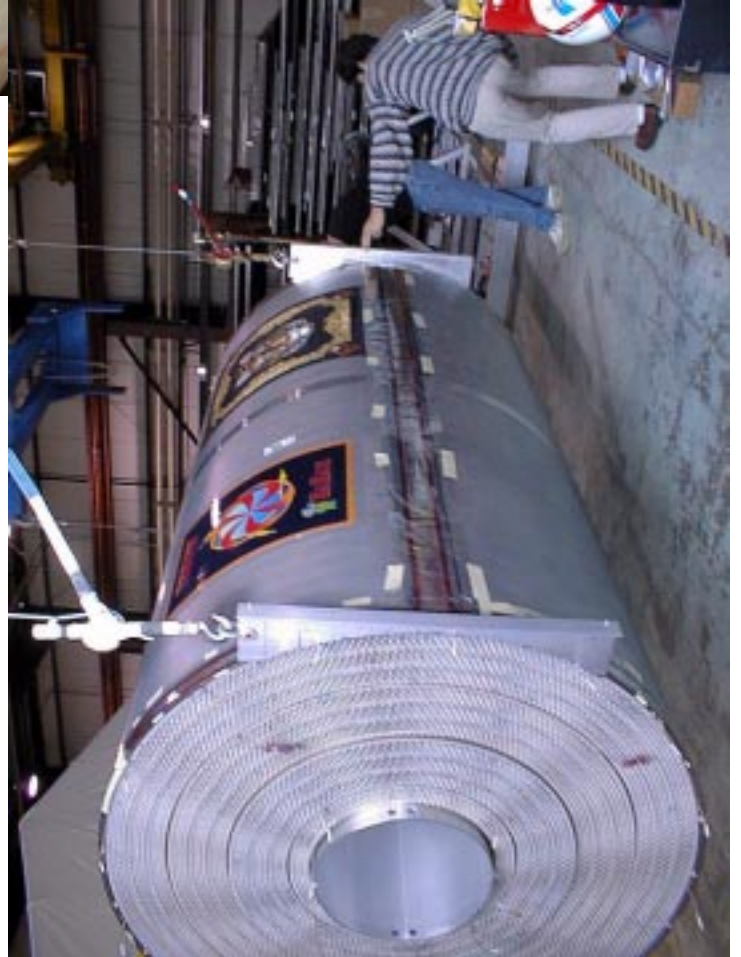
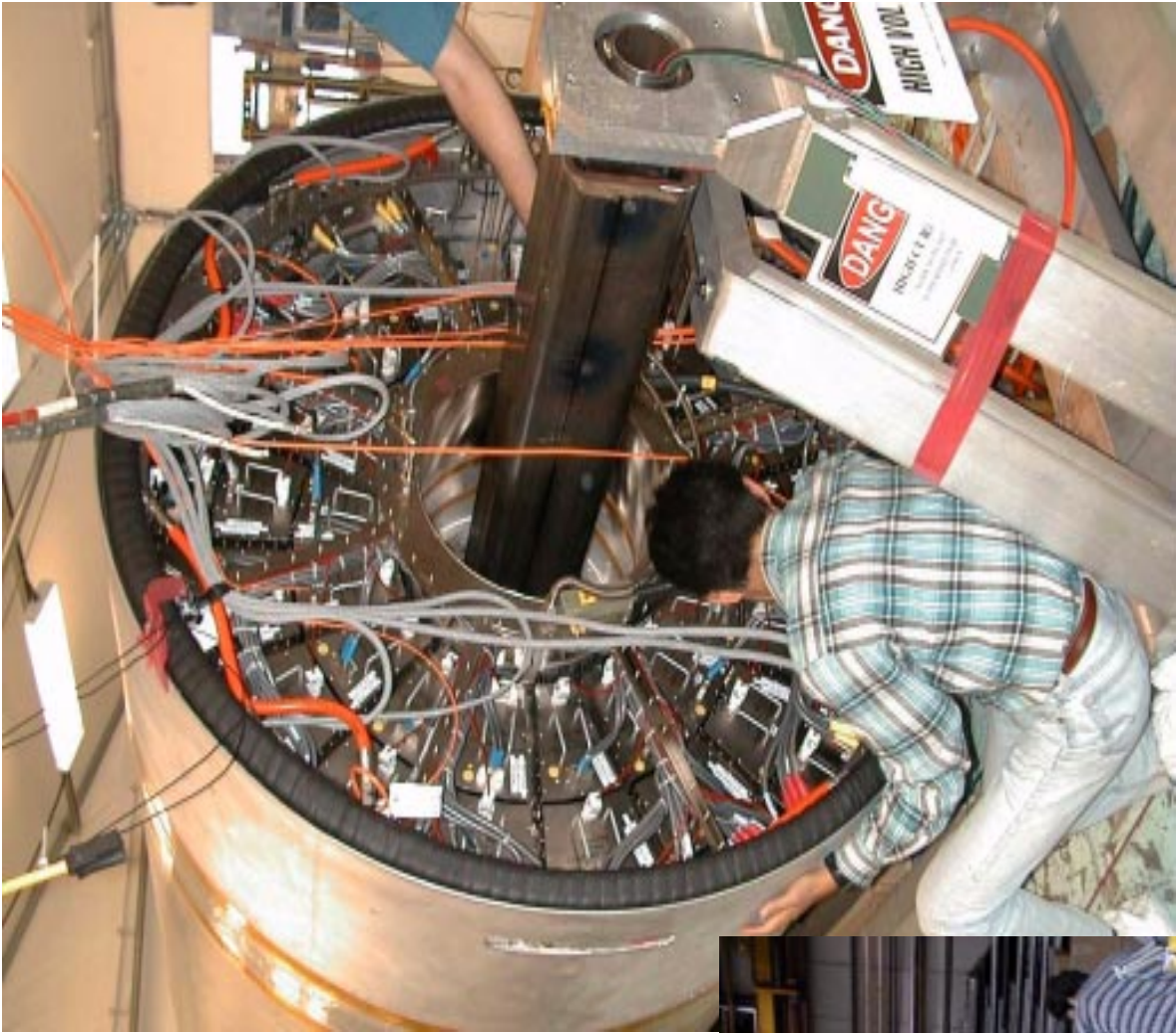


Drift Cell Characteristics

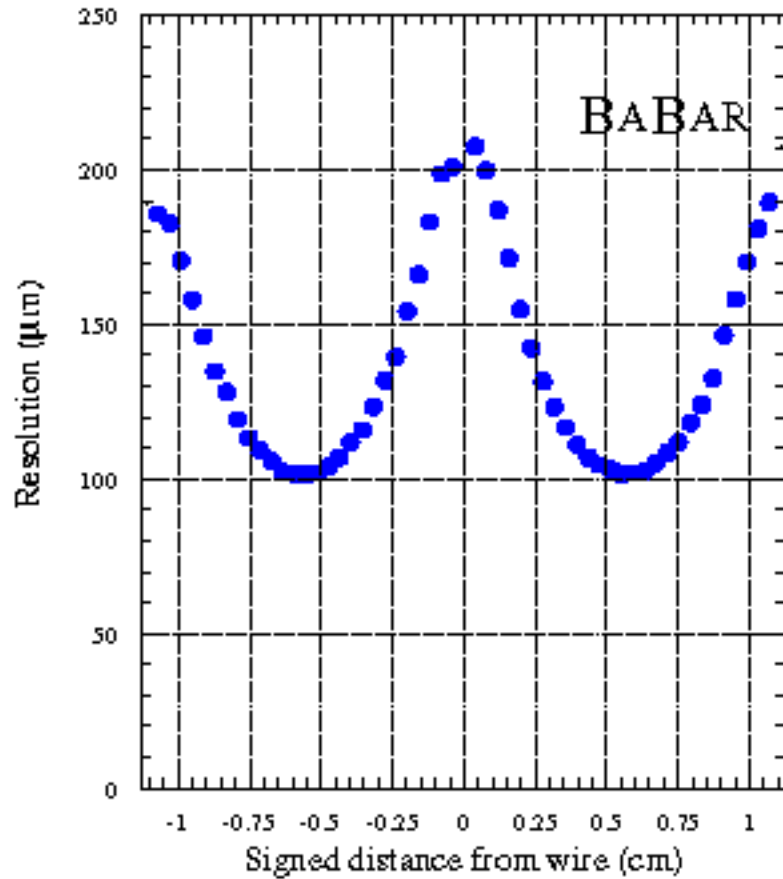
- Nominal 80:20 helium-isobutane gas mixture
 - Low-mass gases able to achieve sub-100 μm position resolutions
 - Low multiple scattering required by soft B decay products
 - dE/dx performance comparable to argon-based mixtures
- Small Lorentz angle should lead to good cell efficiency
 - Modest entrance-angle dependence to STR
- Performance confirmed by measurements with full-length prototype

HEX2 - Wire 108 Isooctane event 50.ms



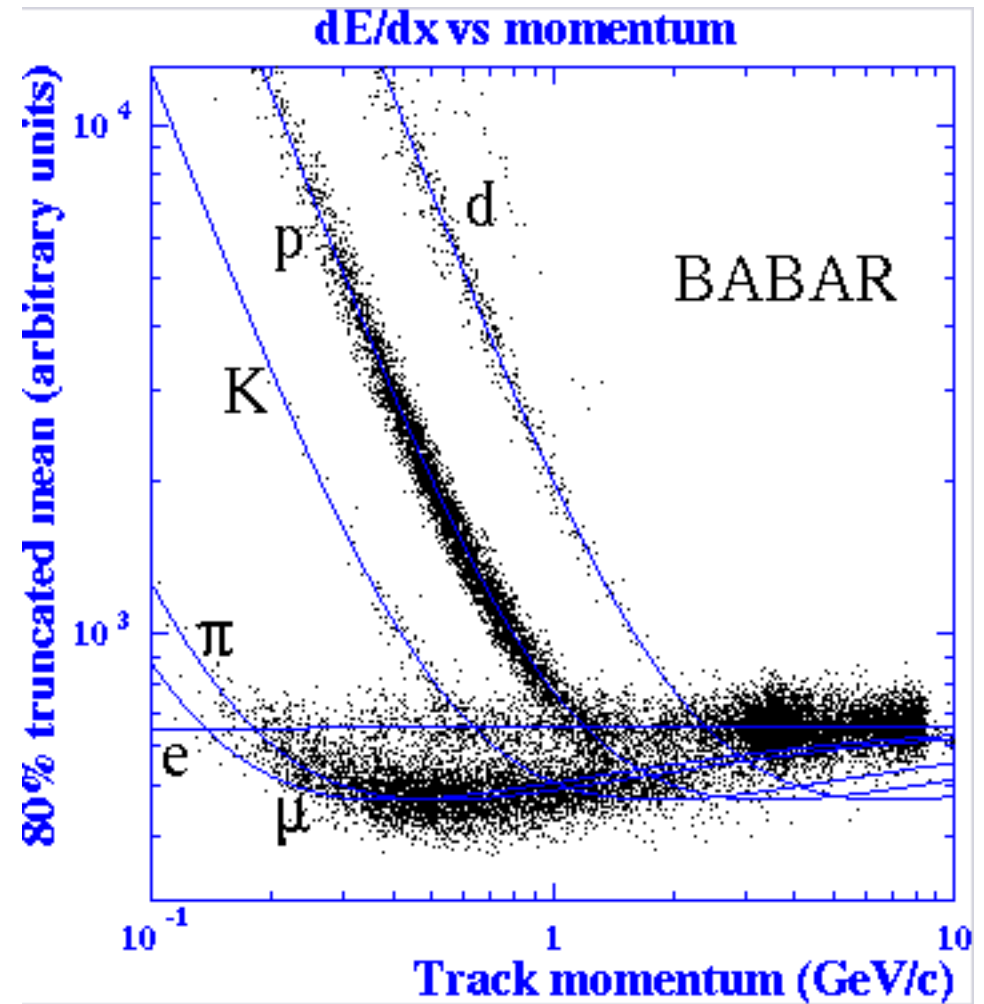


Drift Chamber Hit Resolution



dE/dx vs momentum
 π/k 2 σ separation up to
700 MeV

DCH hit resolution ~ 140 mm

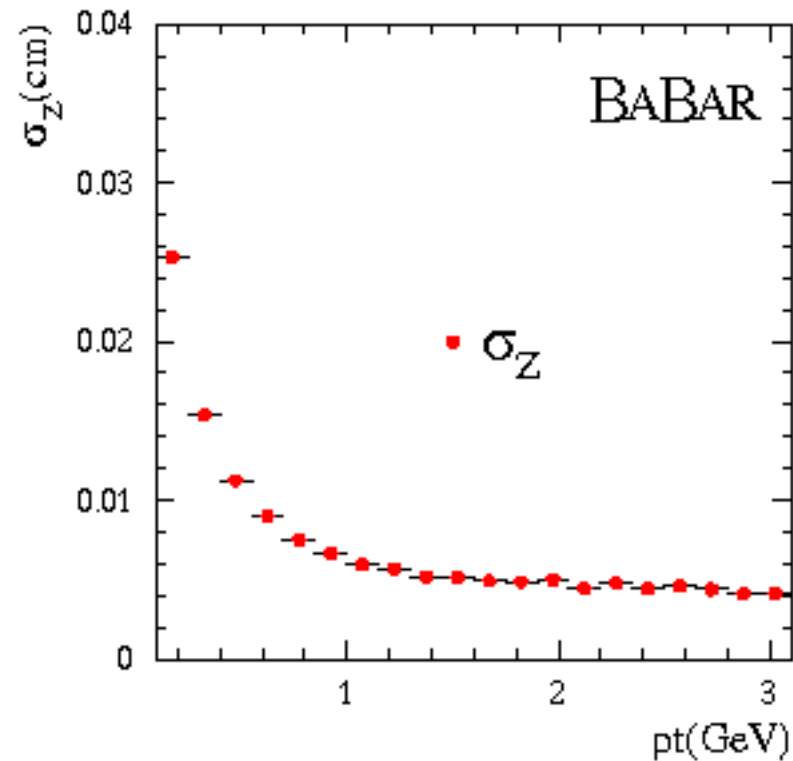
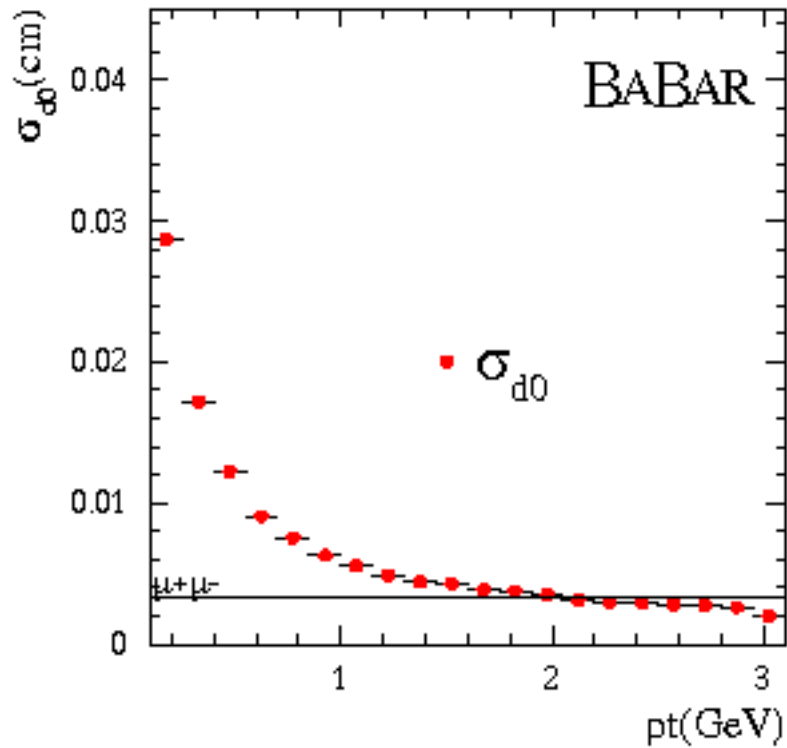
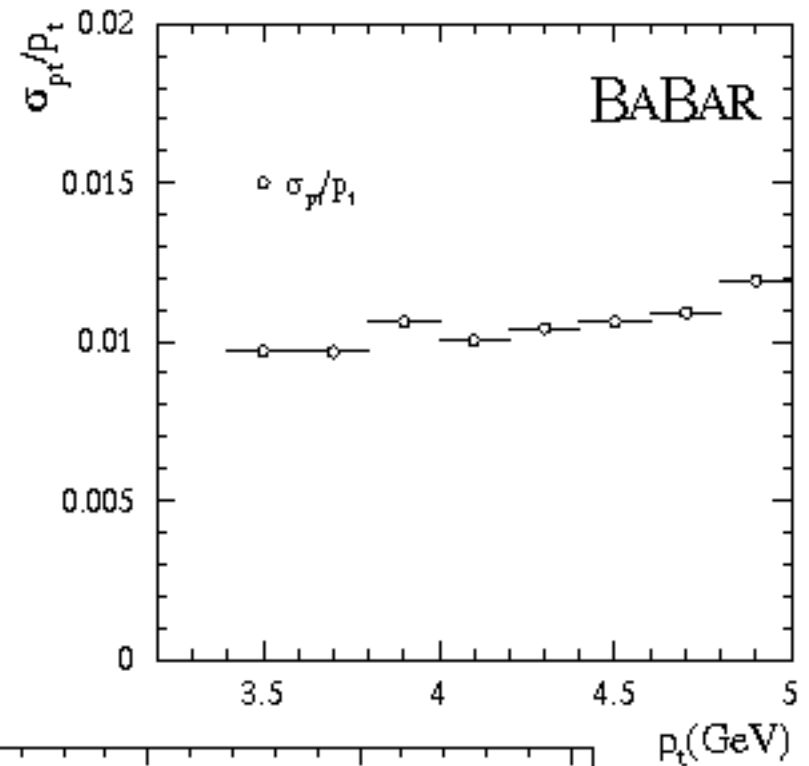


Tracking:

$$\sigma_{Pt}/P_t \sim 1\% \text{ @ } 3 \text{ GeV} \rightarrow$$

doCA:

asymptotic resolution $\sim 35 \mu\text{m}$



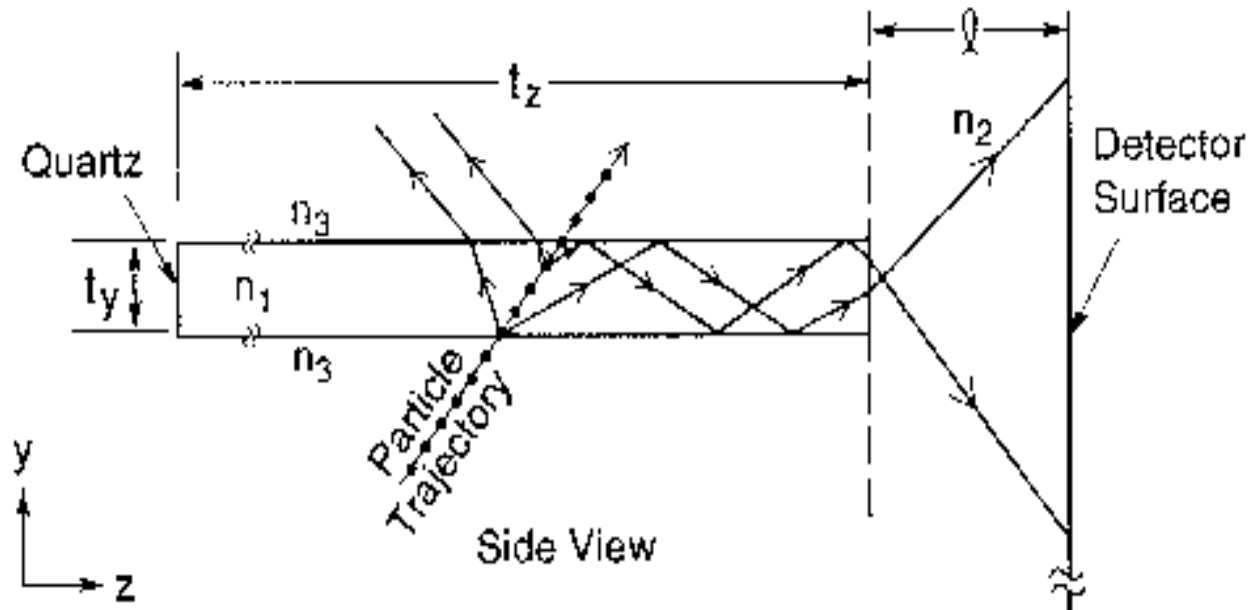
Detector for Internally Reflected Light

Ring imaging Cherenkov detector based on total internal reflection.

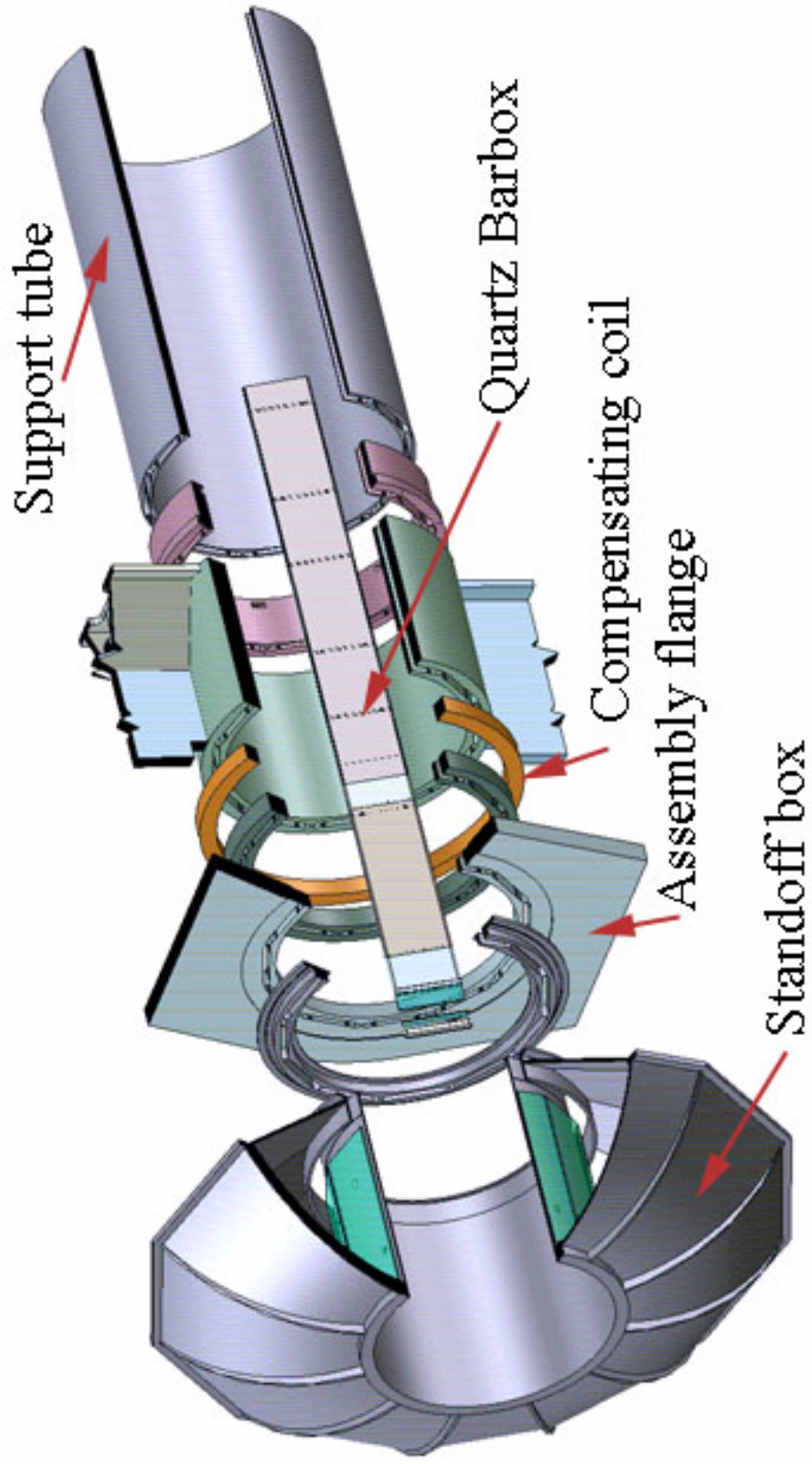
Uses long, rectangular bars made from synthetic fused silica ("quartz") as both radiator and light guide.

A charged particle traversing a DIRC quartz bar with velocity β produces Cherenkov light if $\eta\beta > 1$.

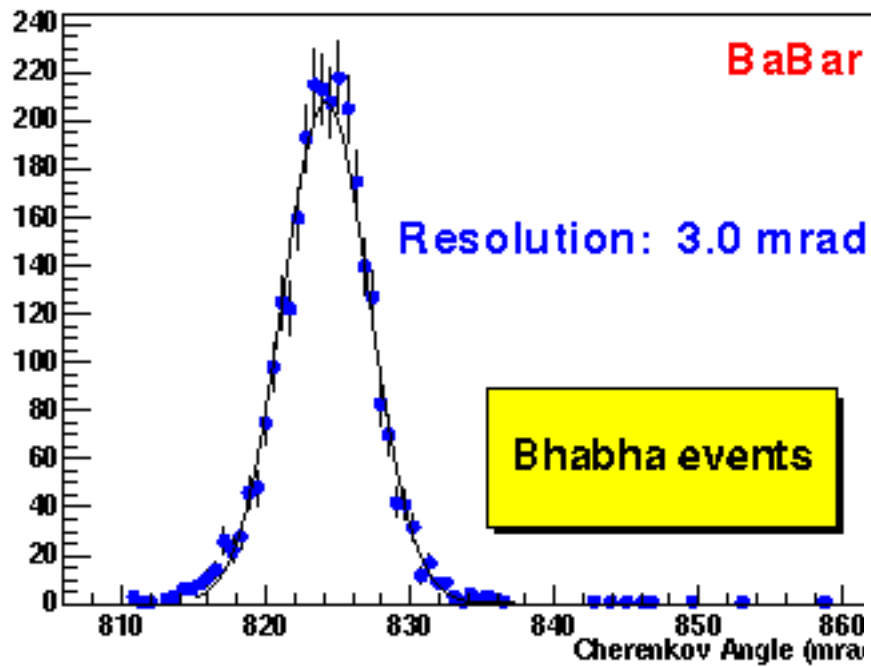
Through internal reflections, the Cherenkov light from the passage of a particle is carried to the ends of the bar and to an array of 11,000 conventional 2.5 cm-diameter phototubes.



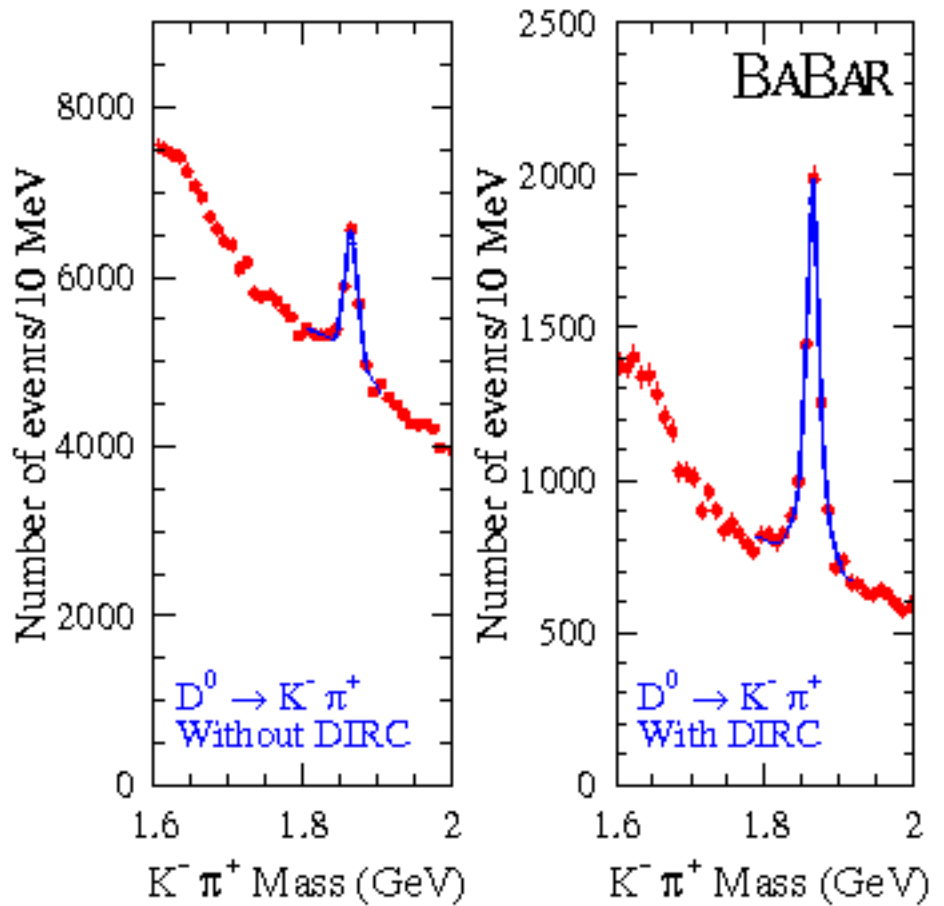
The high optical quality of the quartz preserves the angle of the emitted Cherenkov light. The measurement of this angle, in conjunction with knowing the track angle and momentum from the drift chamber, allows a determination of the particle mass.

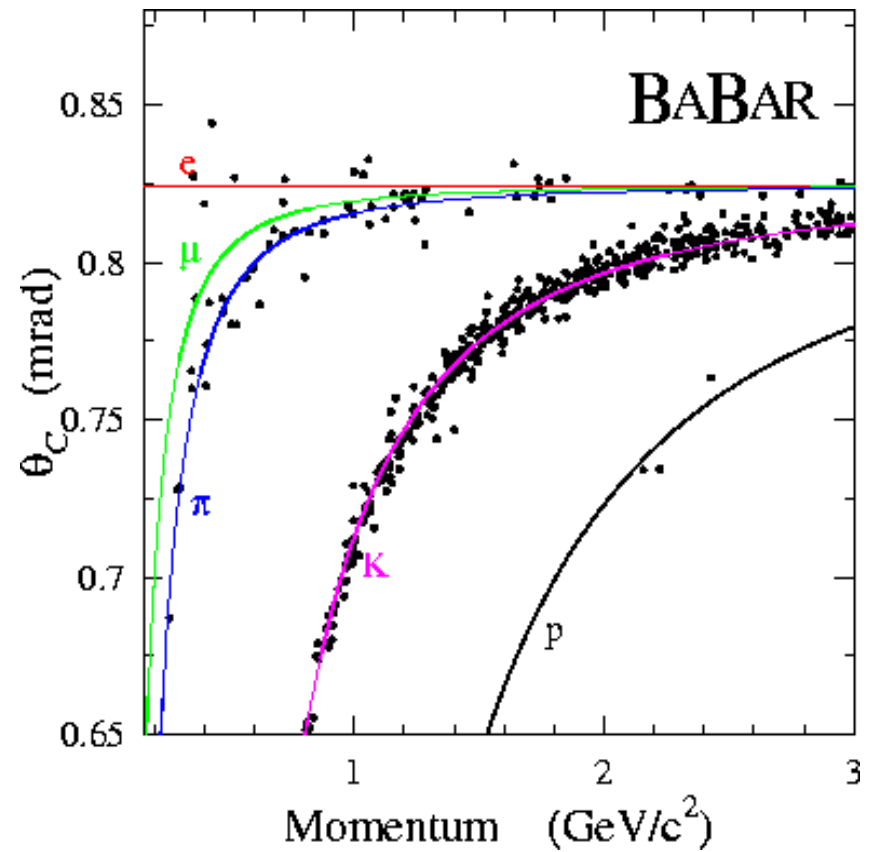
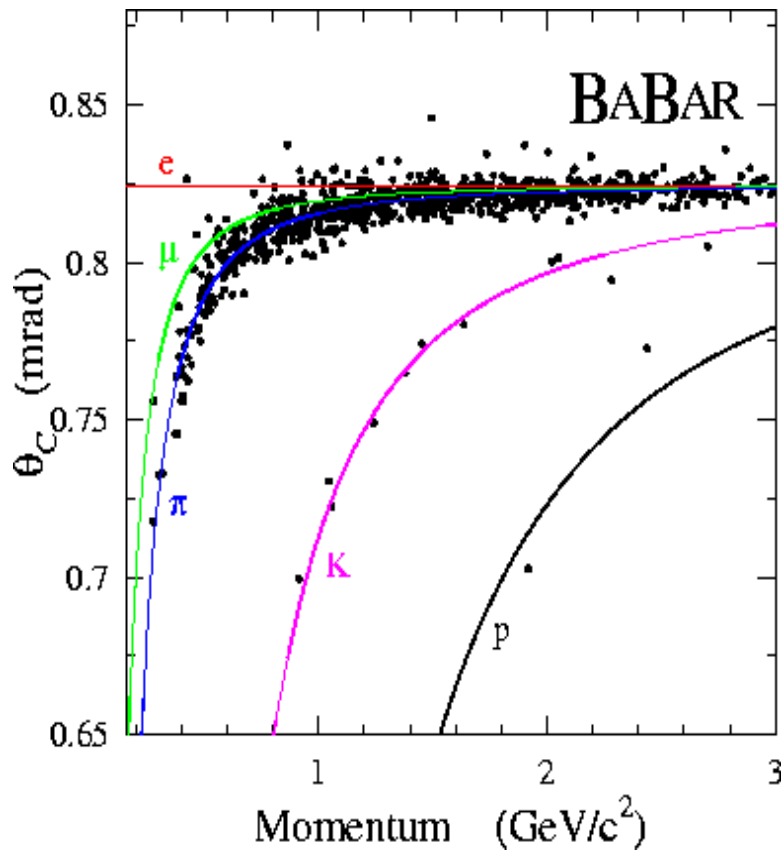


Cherenkov Resolution per Track for DIRC



Impact on D^0 purity
Background rejection
factor ~ 5





π and k from $D^0 \rightarrow K^- \pi^+$

D^0 and \bar{D}^0 are tagged reconstructing the decay $D^{*+} \rightarrow D^0 \pi^+$
 K efficiency $\sim 80\%$

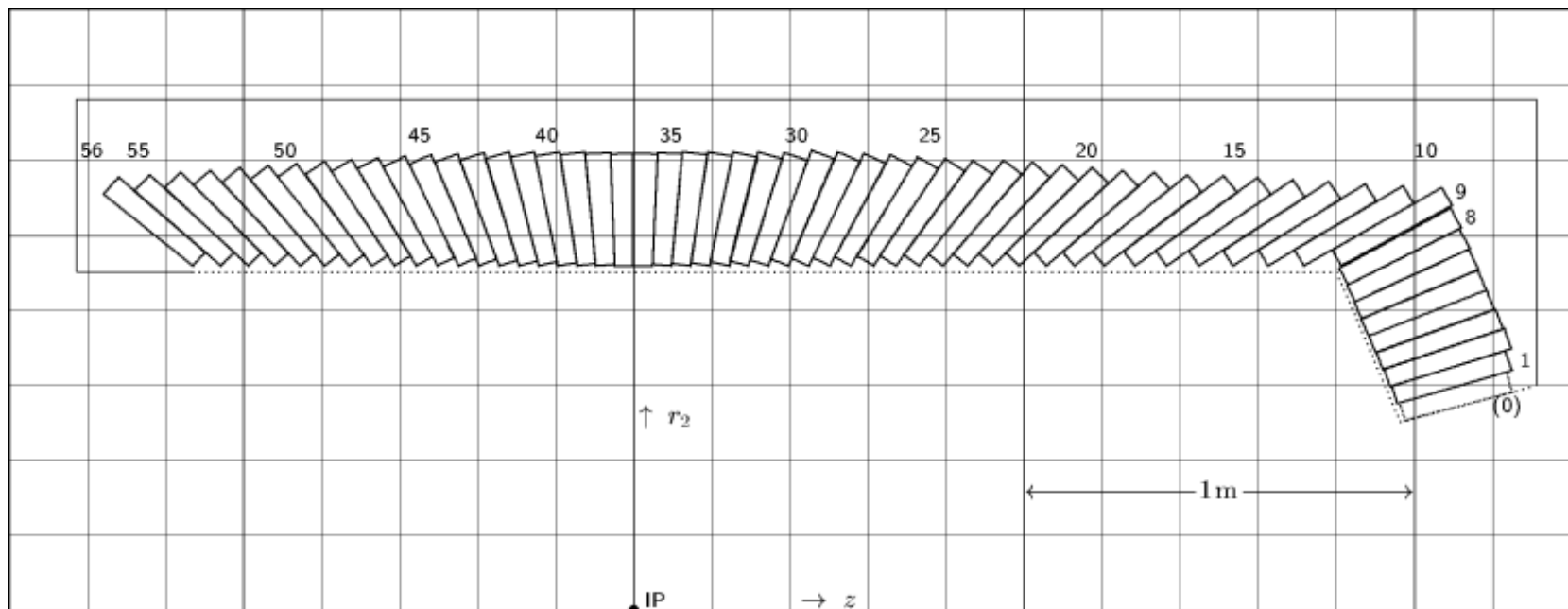
Electromagnetic Calorimeter

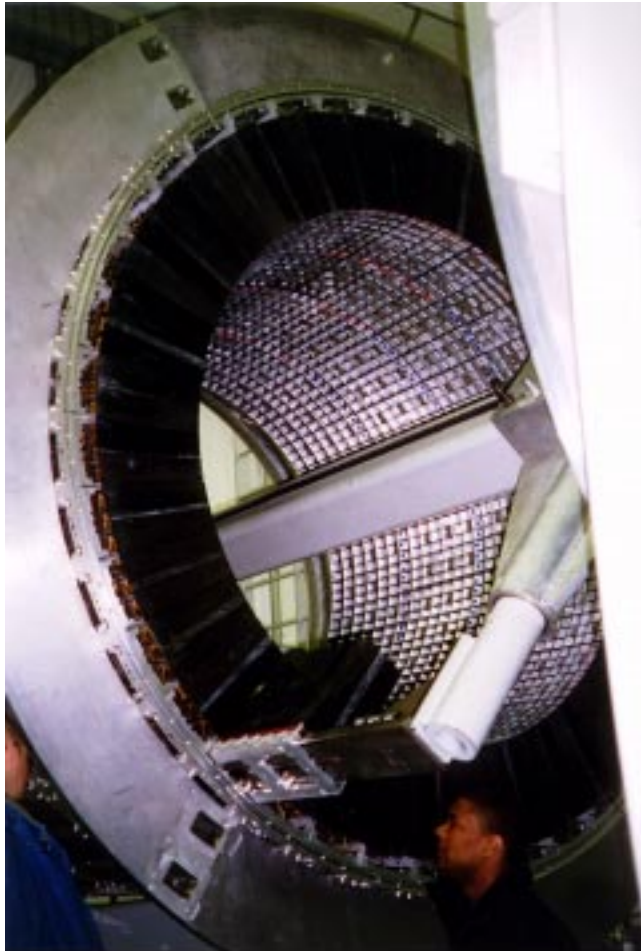
CsI(Tl) crystals

Barrel: 5760 crystals, 48 polar-angle rows, each having 120 identical crystals in azimuthal angle

Endcap: 820 crystals, in 8 theta rings, starting at an inner radius of 55.3 cm from the beam line.

material in front: 0.20-0.25 X_0



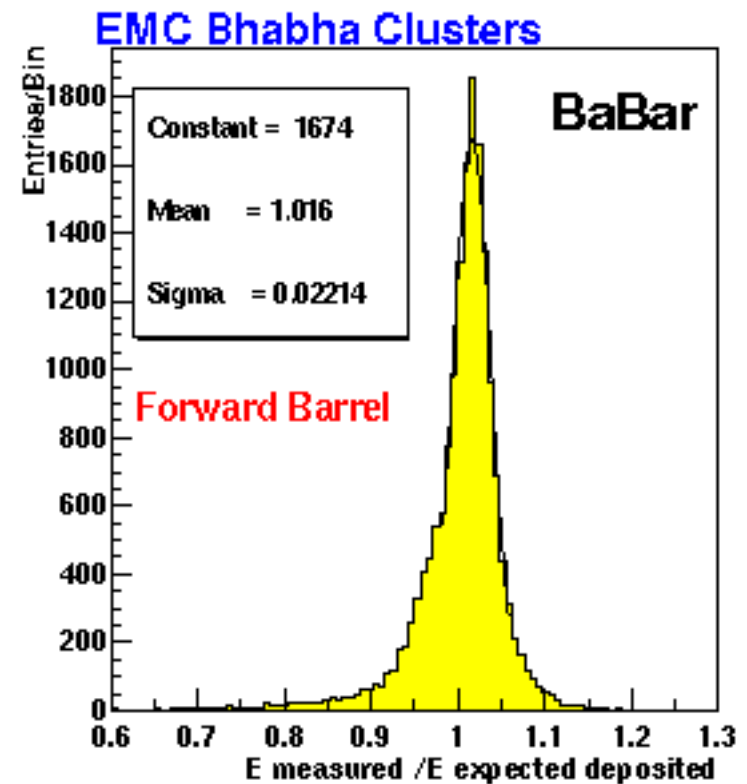


RS_025 Calorimeter - Insertion of last Module 04/13/98

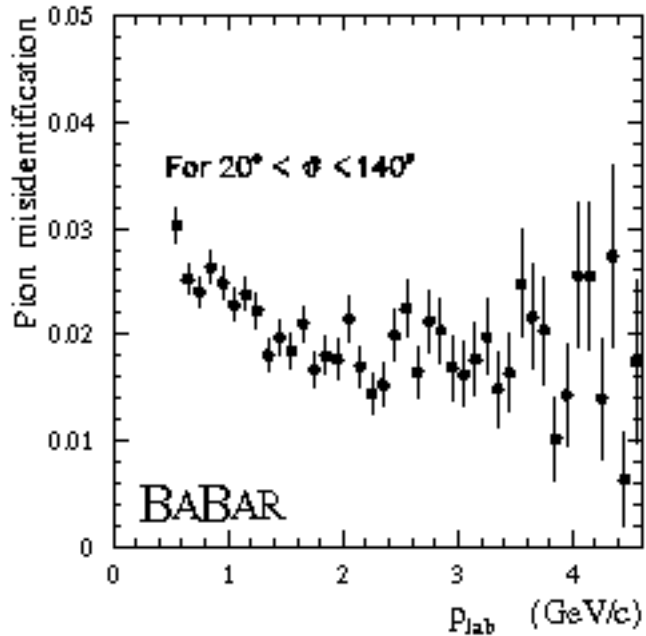
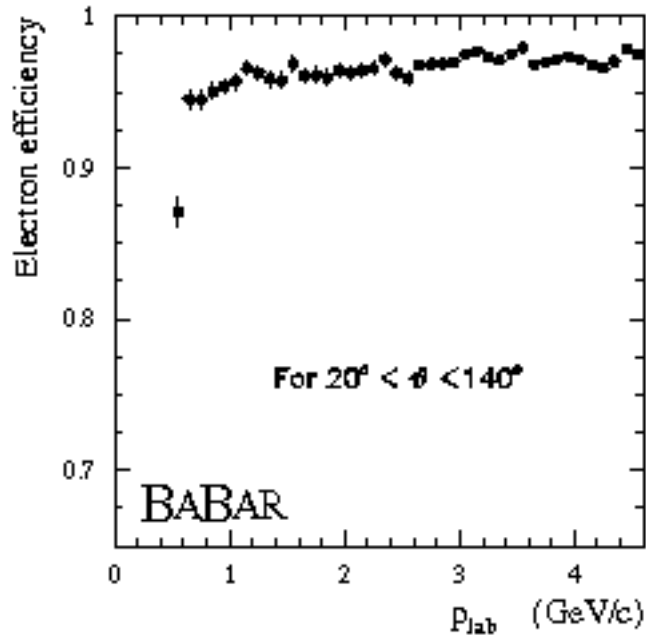
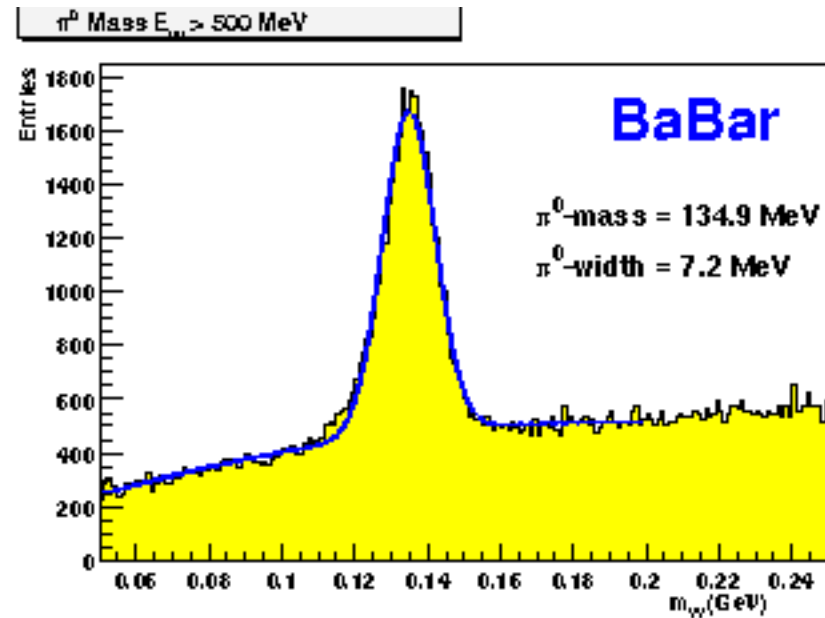
readout by 2 large area photodiodes

liquid source for calibration in front of the crystals

expected energy from the track angle



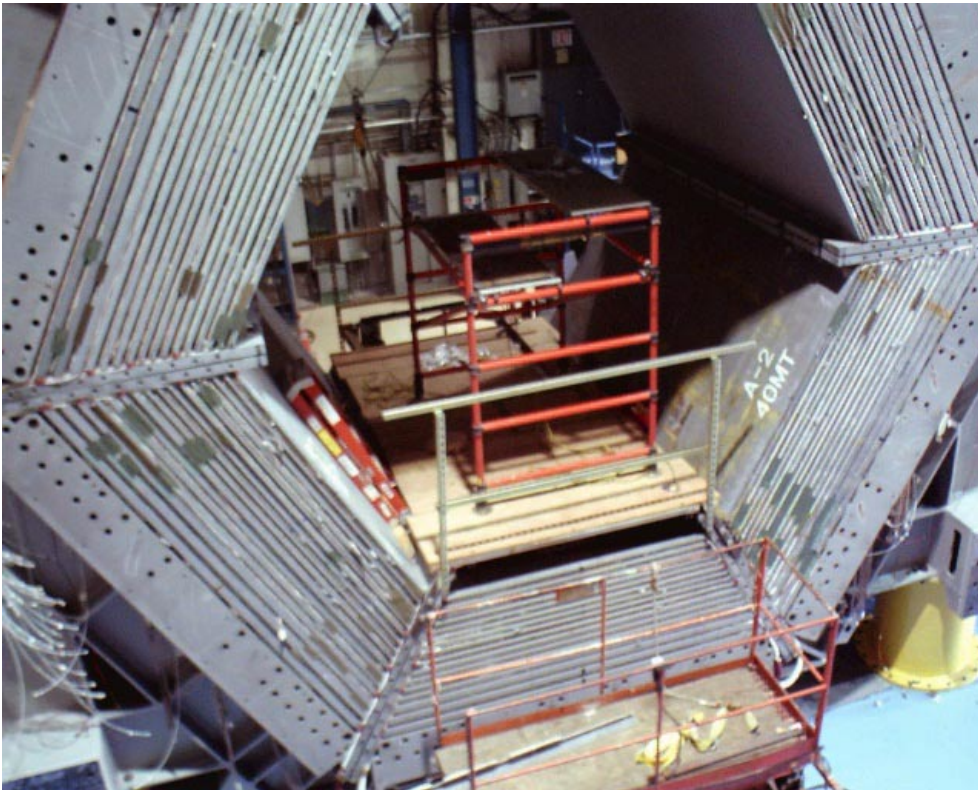
π^0 reconstruction expected resolution: 6.5 MeV



electron ID:
 $\epsilon \sim 95\%$
 π misID $\sim 2\%$

Instrumented Flux Return

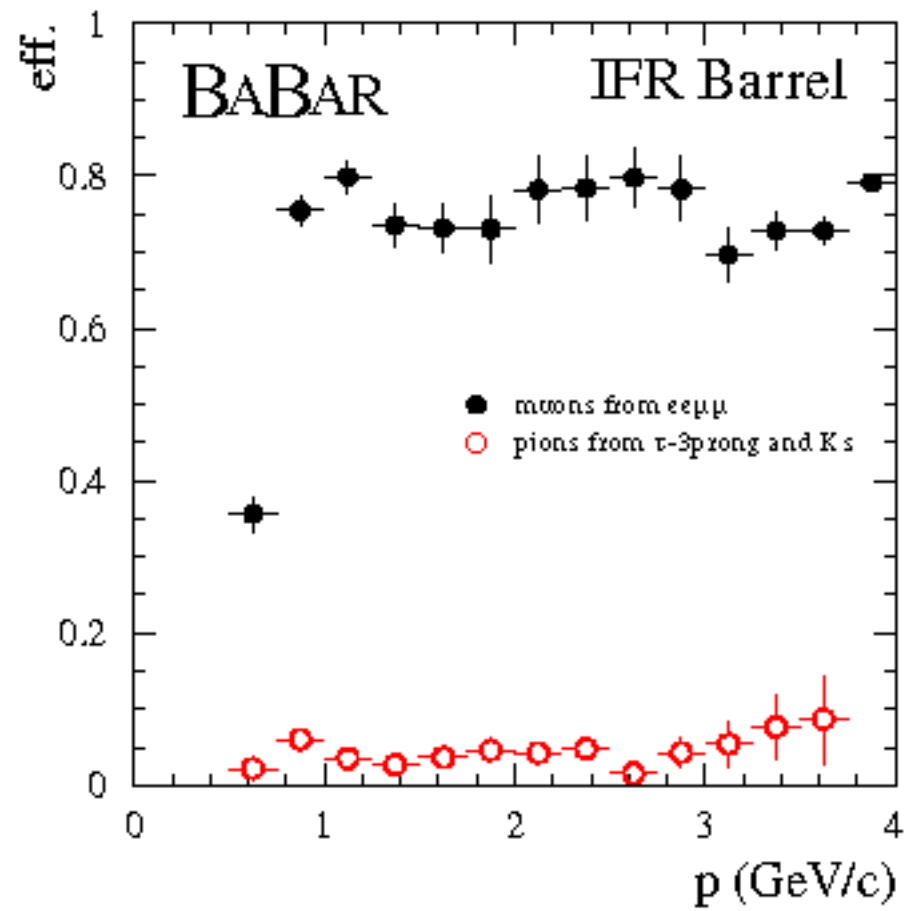
Bakelite-based Resistive Plate Chambers sandwiched between iron plates



Iron segmentation optimized for μ id and K_1 reconstruction

2 double-layer cylindrical RPC inside the coil

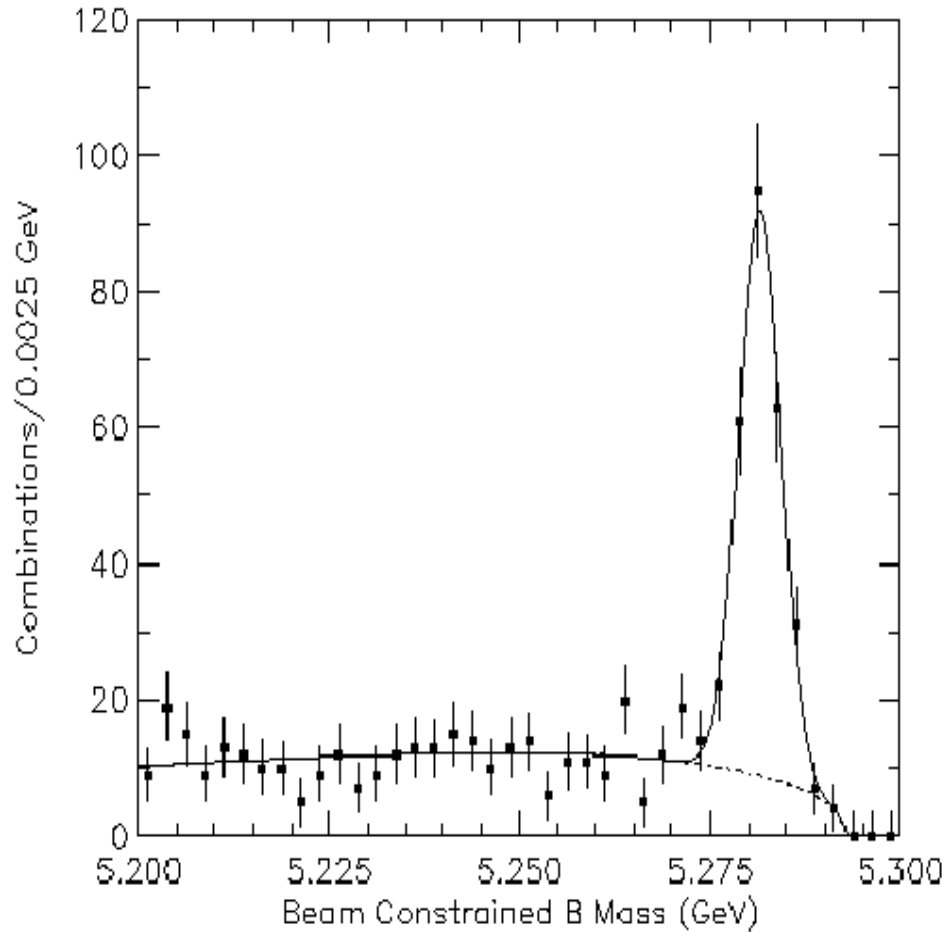
Heating problems leading to high current in the RPC fixed adding water cooling



muon id efficiency (and fake rate from π)

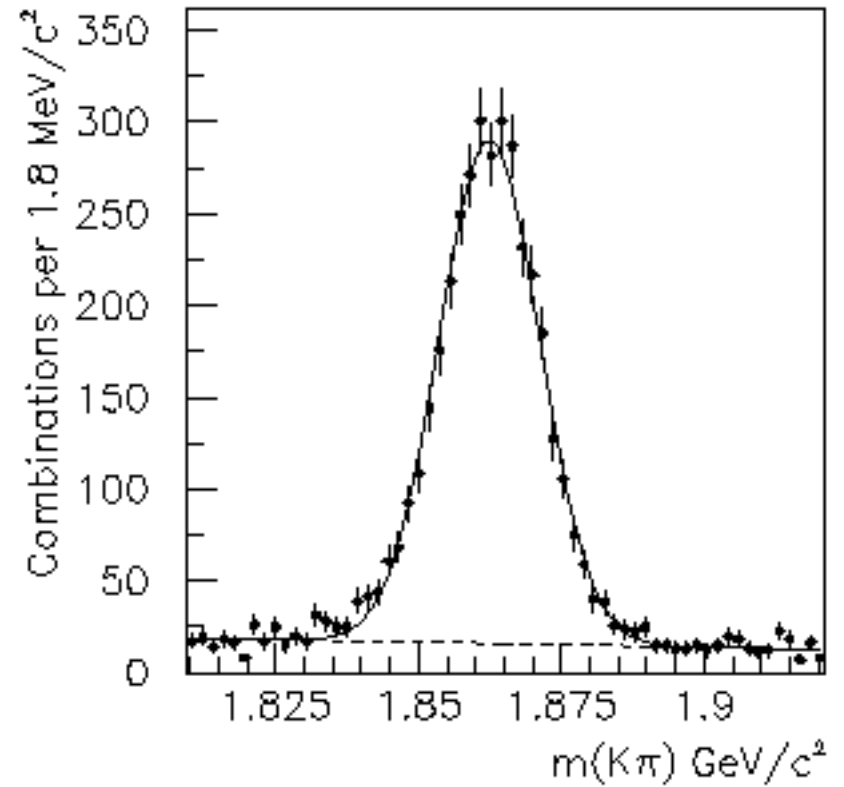
Inclusive Reconstruction:

$D^0 \rightarrow K^- \pi^+$
 $\sigma = 8.8 \text{ MeV}$



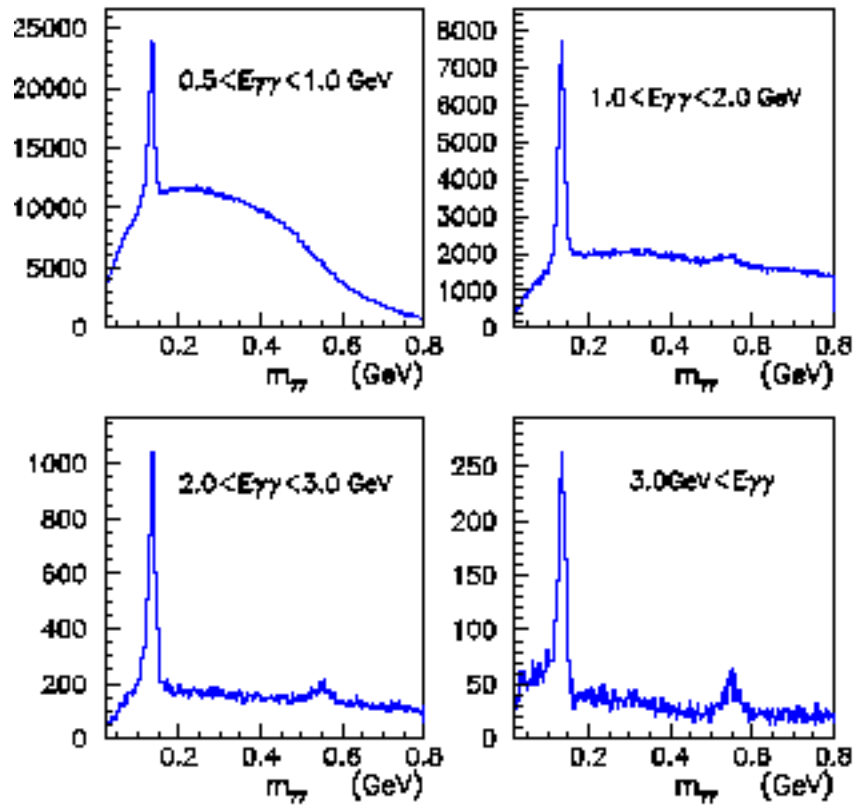
$D^0 \rightarrow K^- \pi^+$

BaBar



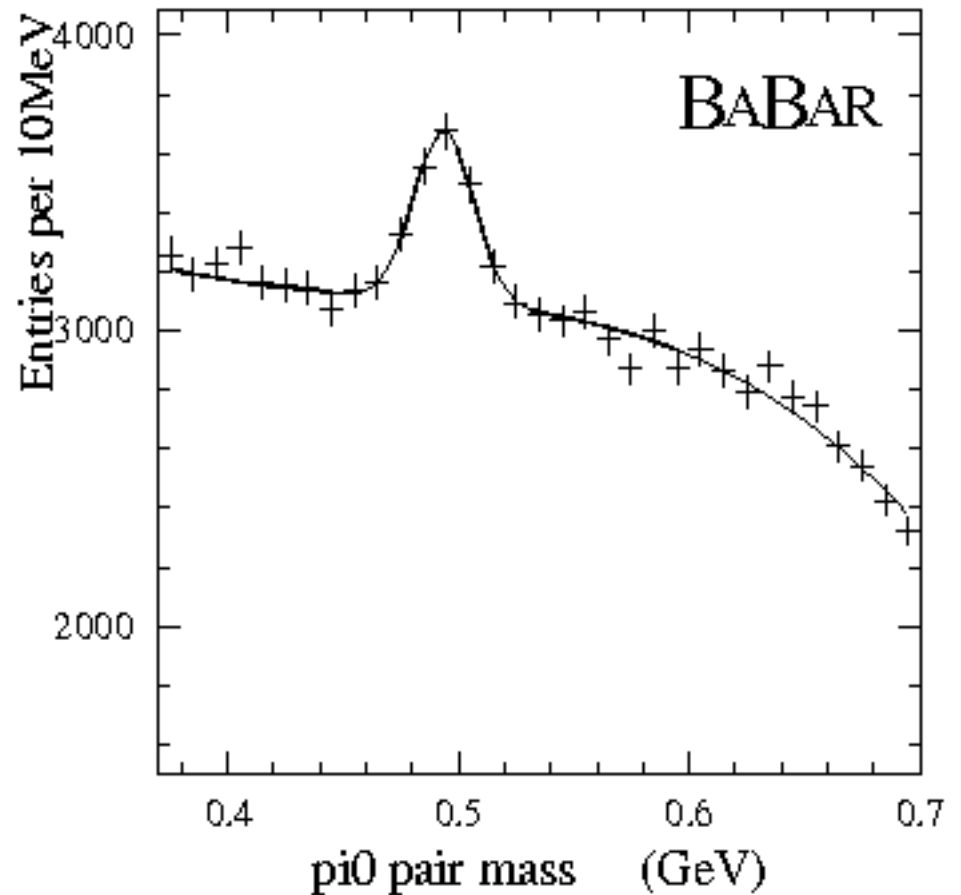
$B^0 \rightarrow D^{(*)} n\pi$
 $\sigma \sim 3 \text{ MeV}$

BABAR



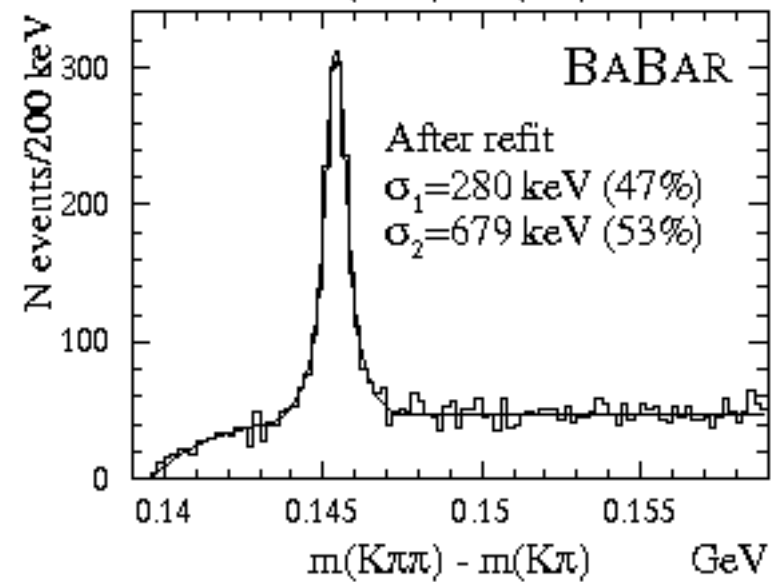
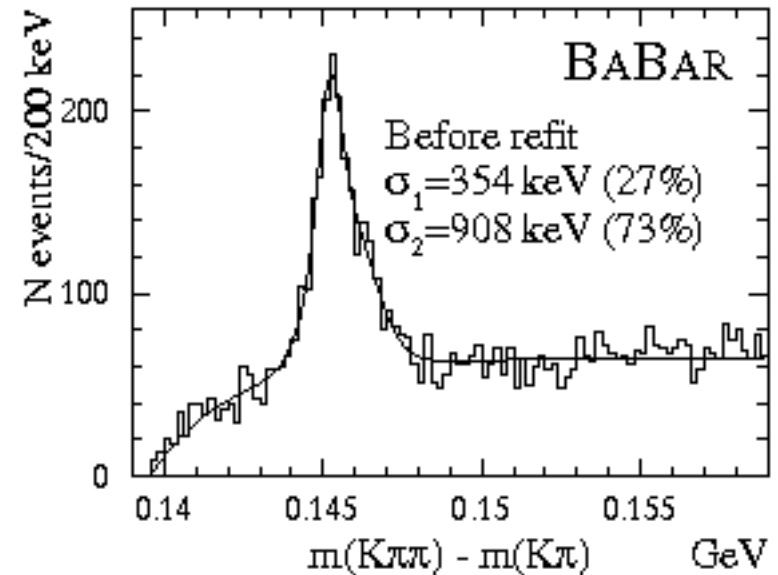
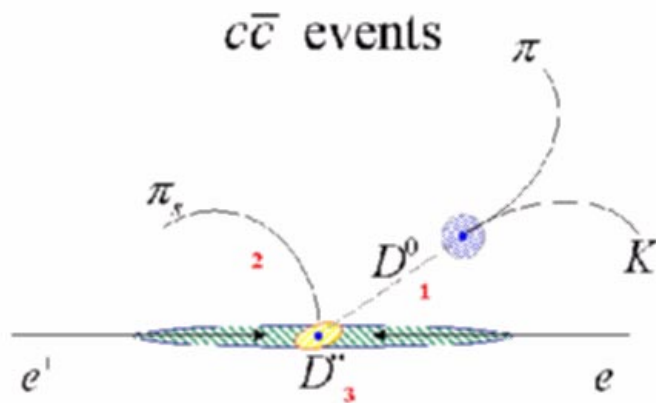
← π^0 and η in $\gamma\gamma$ mass

$K_S \rightarrow \pi^0\pi^0$ →
 K_S energy > 1.5 GeV

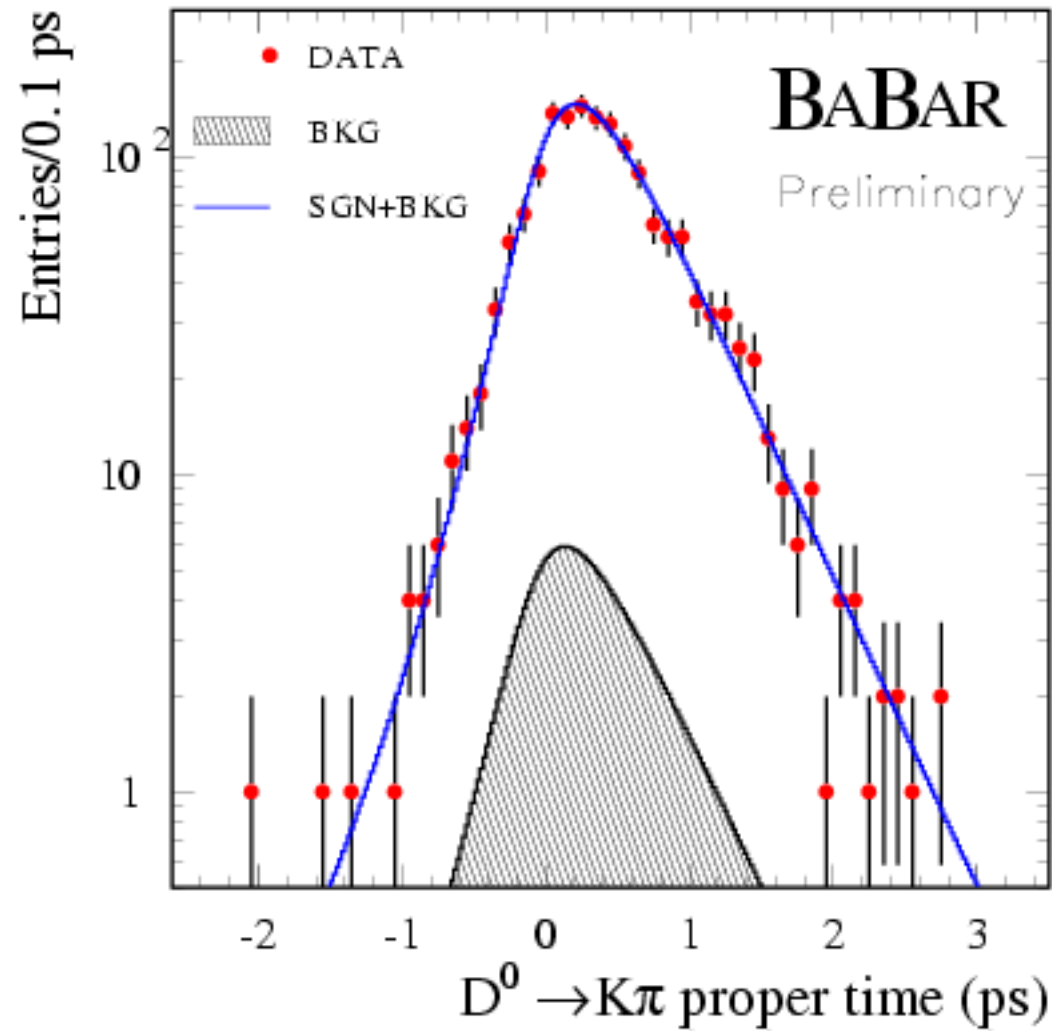


Vertexing Performances

resolution is improved
by using **kinematic constraints**
(masses, directions, beam spot position)



D^0 lifetime consistent with the world average



Example of CP analysis from BaBar

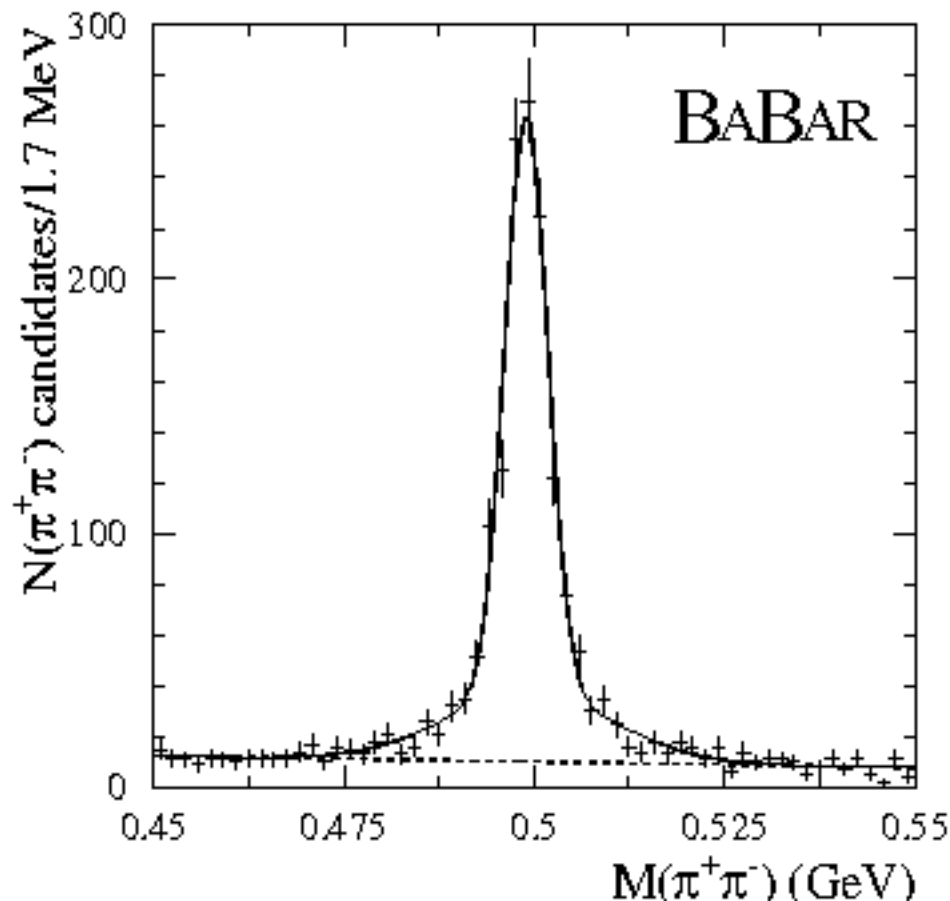
We have looked at BaBar performances w.r.t. the crucial elements of a CP analysis

We are now ready to discuss an example:

$$B \rightarrow J/\psi K_S$$

K_s reconstruction:

- pair tracks with opposite charge
- perform a vertex fit (usually apply a cut on $P(\chi^2)$)
- add some cuts to reduce combinatorial background:
angle between direction of flight and direction of beam spot
 P_t of daughters w.r.t. the K_s flight direction



$K_s \rightarrow \pi^+\pi^-$

double gaussian fit
70% first gaussian with
2.8 MeV resolution

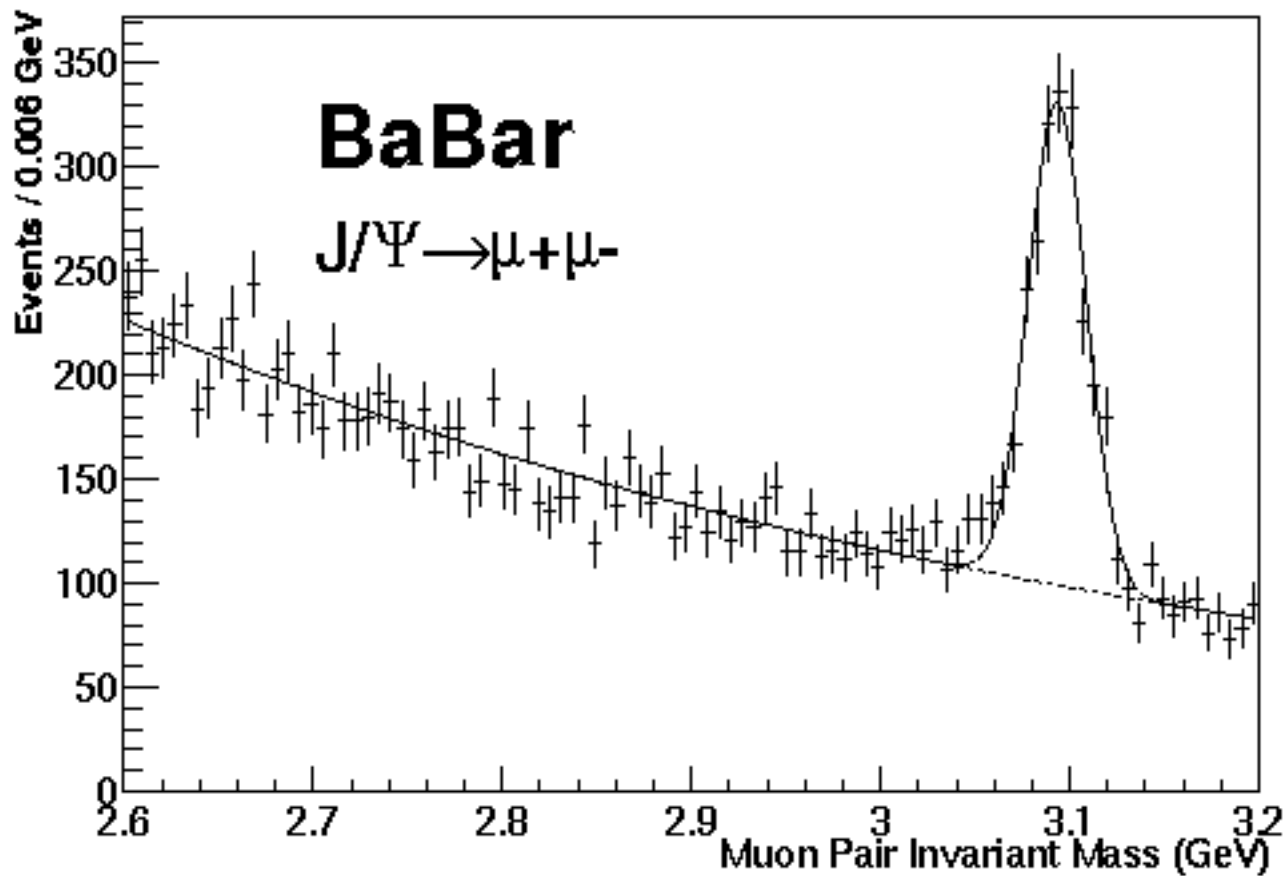
J/Ψ reconstruction

J/Ψ → μμ

- **require tracks to be muons**
- **p* (J/Ψ) < 2 GeV**
- **prob(χ^2) > 1%.**

J/Ψ → ee

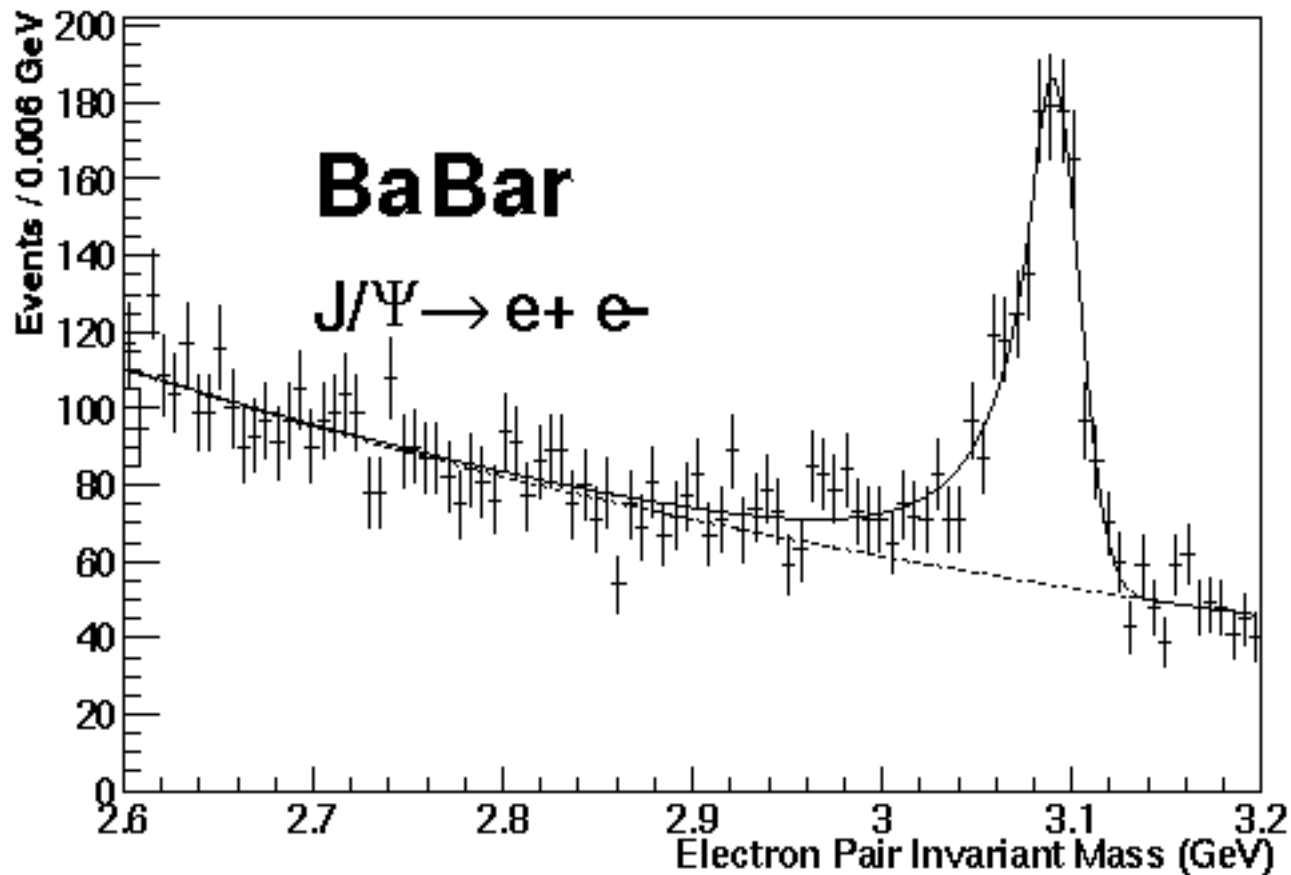
- **require tracks to be electrons**
- **Apply Brehmsstrahlung recovery**
- **p* (J/Ψ) < 2 GeV**
- **prob(χ^2) > 1%**



Data set: 1.9 fb^{-1} ~ 1500 events

$M = 3093.4 \text{ MeV}$ $\sigma = 15.3 \text{ MeV}$

efficiency ~ 64%



Data set: 1.9 fb^{-1} ~ 1200 events

$M = 3090 \text{ MeV}$ $\sigma = 14 \text{ MeV}$

efficiency ~ 52%

Bremsstrahlung recovery is applied on both daughters

B reconstruction

Take advantage of kinematics

In the $\Upsilon(4S)$ rest frame:

$$\Delta E = E_{\text{exp}} - E_{\text{meas}}, m_B = \sqrt{(E_{\text{exp}}^2 - p_{\text{meas}}^2)}, E_{\text{exp}} = \sqrt{s}/2$$

For signal events:

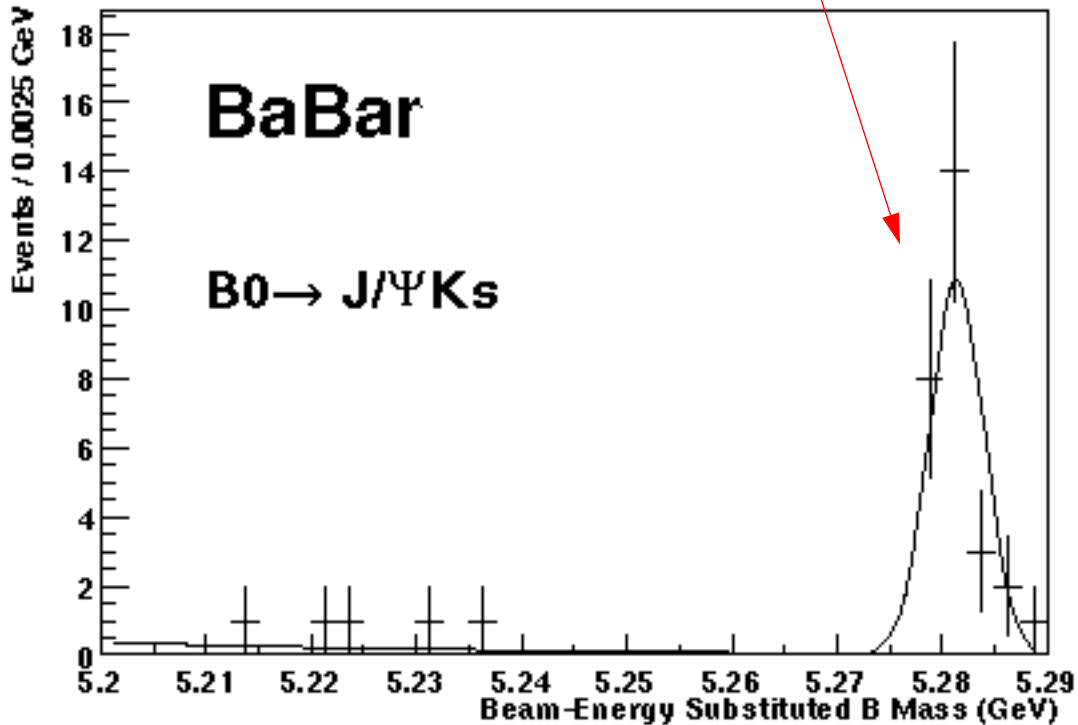
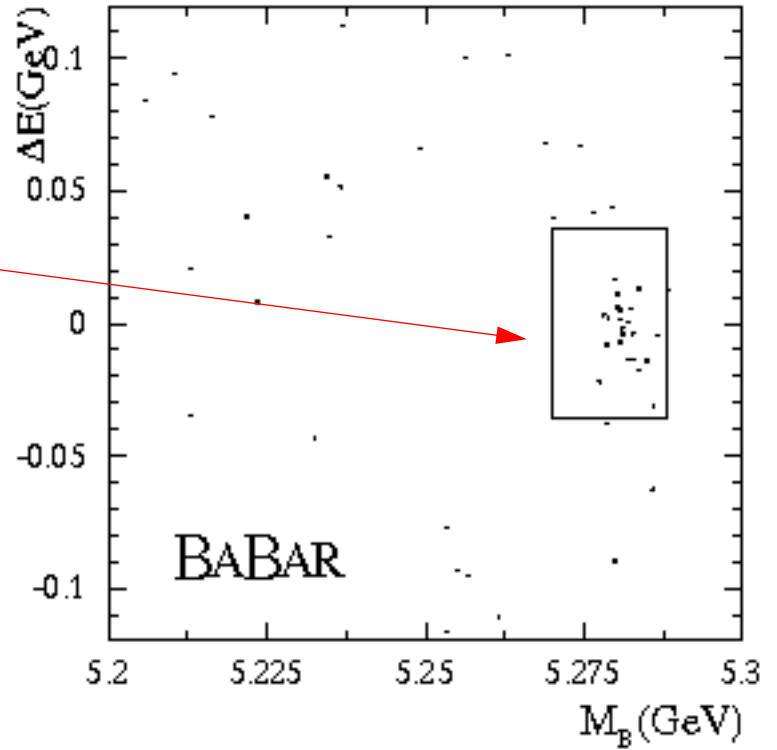
- ΔE peaks at 0
- m_B (beam energy substituted mass) peaks at the B mass

Study signal and background in ΔE vs m_B plot

28 +/- 5 J/Ψ K_s events

π⁺π⁻
I⁺I⁻

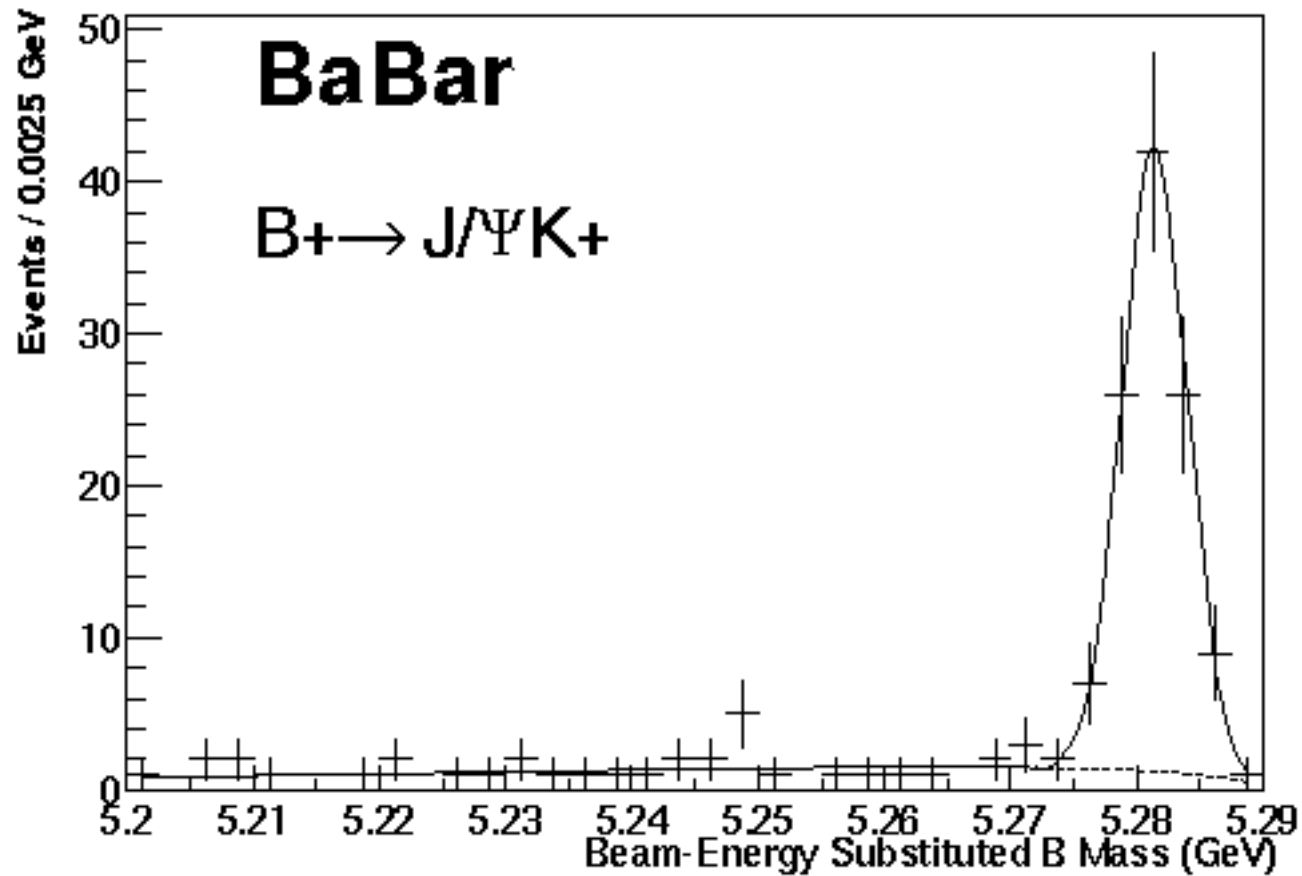
M_B = 5281.4 MeV



Cross check:

109 \pm 11 $B^+ \rightarrow J/\psi K^+$ events

$M_B = 5281.4 \text{ MeV}$



Tagging

the other B has to be identified as a B^0 or an \bar{B}^0

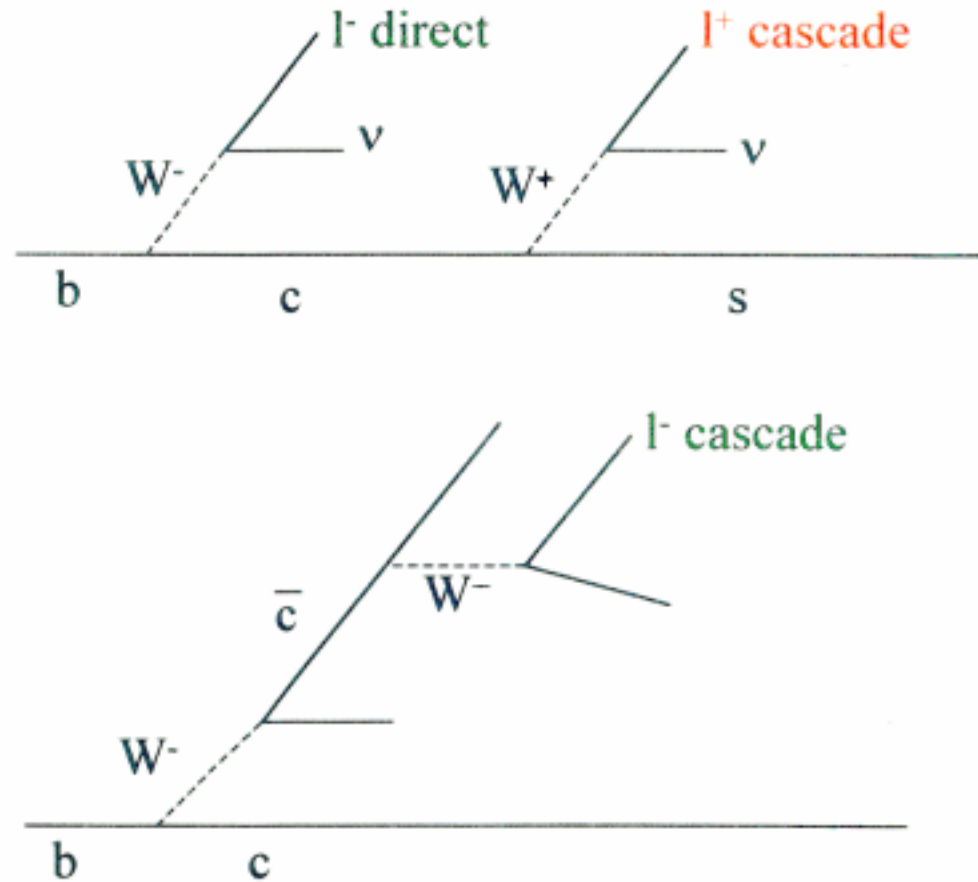
One can use:

- the sign of lepton from B decays
- the sign of kaon from B decay products
- lepton-kaon
- jet charge (no PID used)

to be evaluated the mis-tag probability for each method!

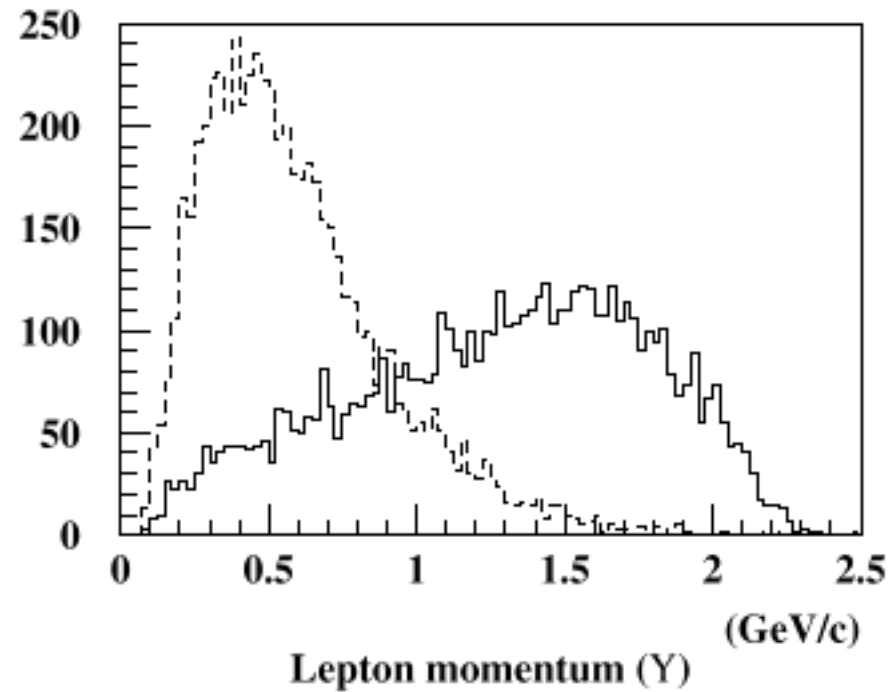
Example: Lepton Tagging

$\text{Br}(B \rightarrow l X) \sim 10\%$



Cascade decays can give lepton of both sign

Clean sample of leptons from b decays cutting on momentum



Want:

- **high efficiency:** maximize the fraction of event that fall in a tagging category
- **high purity:** minimize fraction of wrong tag:
the measured asymmetry is related to the true one by
 $A_{\text{obs}} = D * A_{\text{true}}$ where $D = 1 - 2w$ (w wrong tag probability)

Rather than using a set of cut, assign to each event a probability

The statistical uncertainty in the measured asymmetry for events tagged in a given category c is:

$$\sigma \propto \frac{1}{\sqrt{\mathcal{E}_c^{\text{tag}} \langle s_c^2 \rangle}} \quad \text{where} \quad \langle s^2 \rangle = (1 - 2w)^2$$

Locating decay vertices

for CP decay:

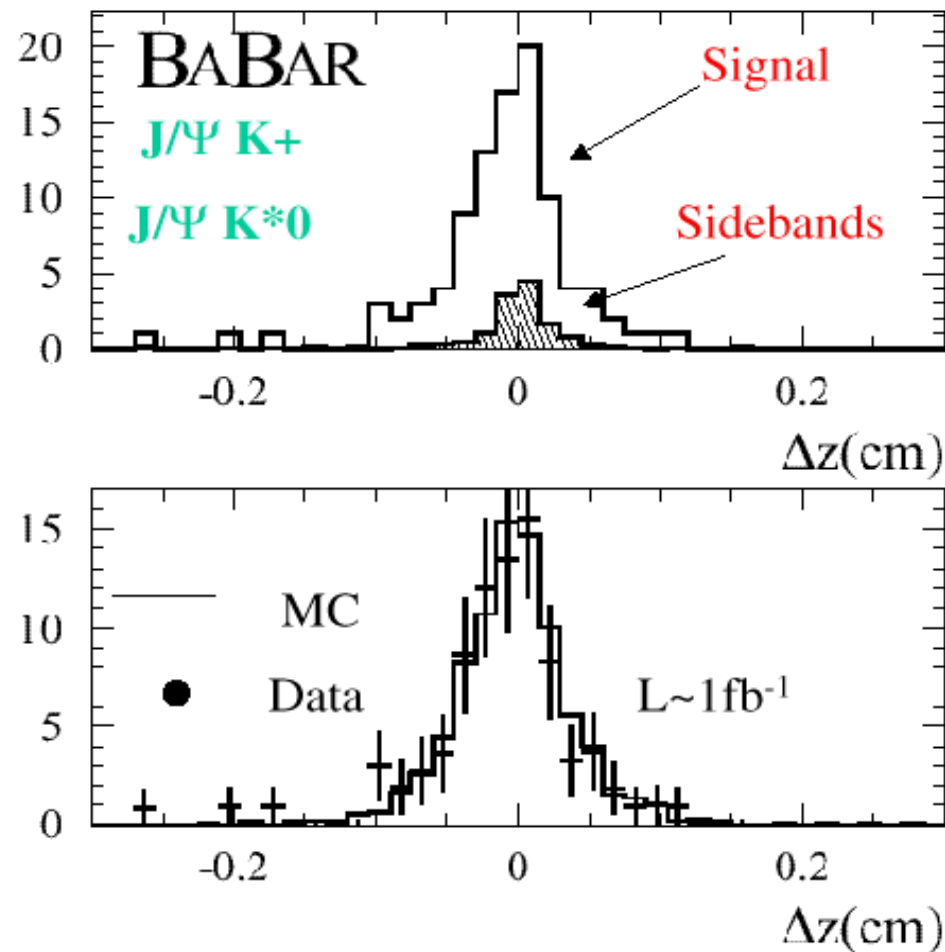
- **the decay is fully reconstructed: perform a vertex fit**

for tag decay:

- **may not have complete decay**
- **in principle can use all remaining tracks, but this will almost certainly include tracks from long lived intermediate particles**
- **use different techniques:**
 - if there is an high energy lepton use point on track closest to IP**
 - otherwise discard badly measured tracks and tracks clearly from secondaries**

We are interested in $t_{CP} - t_{tag}$

We measure Δz $\gamma\beta c(t_{CP} - t_{tag}) \cong z_{CP} - z_{tag} \equiv \Delta z$



Fitting the CP asymmetries

The time dependent rate for $Y(4S) \rightarrow B_{\text{fcp}} B_{\text{tag}}$
can be written as:

$$R_{\pm}(t_{\text{tag}} - t_{CP}) \propto e^{-\Gamma t_{\text{tag}} - t_{CP}} [1 \pm A \sin(\Delta m(t_{\text{tag}} - t_{CP})/\Gamma) \pm B \cos(\Delta m(t_{\text{tag}} - t_{CP})/\Gamma)]$$

“+” sign if the recoiling B_{tag} is a B

“-” sign if the recoiling B_{tag} is a \bar{B}

$$A = -\frac{2\text{Im}\lambda_f}{1 + |\lambda_f|^2}, \quad B = \frac{1 - |\lambda_f|^2}{1 + |\lambda_f|^2}$$

The observed measurements are smeared by the finite vertex resolution.

Assuming gaussian errors, the observed distribution becomes:

$$f_{\pm}(\Delta z = \Delta t/(\gamma\beta c)) = \int_{-\infty}^{\infty} e^{-(t-\Delta t)^2/2\sigma^2} e^{-\Gamma|t|} \cdot [1 \pm A \sin(\Delta mt'/\Gamma) \pm B \cos(\Delta mt'/\Gamma)] dt'$$

There are not pure sample of B or \bar{B} tags

We measure the probability b (\bar{b}) that the recoil tag is B (\bar{B})

The probability of one CP events become:

$$P = b e^{-\Gamma t} [1 + A \sin \Delta m t] + \bar{b} e^{-\Gamma t} [1 - A \sin \Delta m t]$$

$$e^{-\Gamma t} [(b + \bar{b}) + (b - \bar{b}) A \sin \Delta m t]$$

Usually the probability b and \bar{b} are measured according to some variable x . The probability distribution becomes:

$$e^{-\Gamma t} [(b(x) + \bar{b}(x)) + (b(x) - \bar{b}(x))A \sin \Delta mt] dxdt$$

and can be rewritten as:

$$f(t, x, A) dxdt = e^{-\Gamma t} [1 + q(x) A \sin \Delta mt] n(x) dxdt$$

where

$$q(x) = (b(x) - \bar{b}(x))/(b(x) + \bar{b}(x))$$

and

$$n(x) = b(x) + \bar{b}(x)$$

Including the vertex resolution:

$$f(t, x, A, \sigma_t) dxdt =$$

$$\left[\int \frac{1}{\sqrt{2\pi\sigma_t}} e^{-\frac{1}{2}\left(\frac{t-t'}{\sigma_t}\right)^2} e^{-\Gamma|t|} [1 + q(x) A \sin \Delta mt'] n(x) dt' \right] dxdt$$

$$f(t, x, A, \sigma) dxdt = [E(t) + Aq(x) S(t)] n(x) dxdt$$

$$E(t) = \int \frac{1}{\sqrt{2\pi\sigma_t}} e^{-\frac{1}{2}\left(\frac{t-t'}{\sigma_t}\right)^2} e^{-\Gamma|t|} dt',$$

$$S(t) = \int \frac{1}{\sqrt{2\pi\sigma_t}} e^{-\frac{1}{2}\left(\frac{t-t'}{\sigma_t}\right)^2} e^{-\Gamma|t|} \sin \Delta mt' dt'.$$

Want value of A that maximize the likelihood:

$$\ln \mathcal{L} = \ln \prod_{i=1}^N f(t_i, x_i, A, \sigma_t) = \sum_{i=1}^N \ln f(t_i, x_i, A, \sigma_t)$$

$$\begin{aligned} \ln \prod_{i=1}^N f(t_i, x_i, A, \sigma_t) &= \sum_{i=1}^N \ln [(1 + Aq(x) S(t) / E(t)) E(t) n(x)] \\ &= \sum_{i=1}^N \ln (1 + Aq(x) S(t) / E(t)) + C . \end{aligned}$$

The uncertainty in the likelihood estimate of A can be calculated from:

$$\frac{1}{\sigma_A^2} = N \int \frac{1}{f} \left(\frac{\partial f}{\partial A} \right)^2 dx$$

One gets:

$$\sigma_A(A, \Delta m/\Gamma, \sigma_t, N, w) = \frac{\sigma_0(A, \Delta m/\Gamma, \sigma_t)}{\sqrt{N} \sqrt{\epsilon} (1 - 2w)}.$$

Including an error due to a symmetric background:

$$\sigma_A(A, \Delta m/\Gamma, \sigma_z, N_S, \epsilon, w, N_B) = \frac{\sigma_0(A, \Delta m/\Gamma, \sigma_z) \sqrt{N_S + N_B}}{\sqrt{\epsilon}(1 - 2w)N_S}$$

- N_S is the number of signal events
- N_B is the number of background events
- σ_0 is the contribution to the error for a single event with perfect tag
- ϵ is the tagging efficiency
- w is the wrong tag probability

With 10 fb^{-1} we expect $\sigma(\sin 2\beta) \sim 30\%$

Conclusions:

BaBar and PEP II are working very well

First results in few weeks at ICHEP 2000 (Osaka, Japan)

Stay tuned for our measurement of $\sin 2\beta$!